DEVELOPMENT OF TITANIUM DIBORIDE LAYER THROUGH SUPERPLASTIC COMPRESSION METHOD

NOR TAIBAH BINTI TAAZIM

DISSERTATION SUBMITTED IN FULFILMENT OF THE REQUIREMENTS FOR THE DEGREE OF MASTER OF ENGINEERING SCIENCE

FACULTY OF ENGINEERING
UNIVERSITY OF MALAYA
KUALA LUMPUR

2016

UNIVERSITY MALAYA

ORIGINAL LITERARY WORK DECLARATION

Name of Candidate: **NOR TAIBAH BINTI TAAZIM**

Registration/Matric No: **KGA110075**

Name of Degree: **MASTER OF ENGINEERING SCIENCE**

Title of Project Paper/Research Report/Dissertation/Thesis ("this Work"):

DEVELOPMENT OF TITANIUM DIBORIDE LAYER THROUGH SUPERPLASTIC COMPRESSION METHOD

Field of Study: **ENGINEERING MATERIALS**

I do solemnly and sincerely declare that:

(1) I am the sole author/writer of this Work;

(2) This Work is original;

(3) Any use of any work in which copyright exists was done by way of fair dealing and for permitted purposes and any excerpt or extract from, or reference to or reproduction of any copyright work has been disclosed expressly and sufficiently and the title of the work and its authorship have been acknowledged in this work;

(4) I hereby assign all and every rights in the copyright to this work to the University of Malaya ("UM"), who henceforth shall be owner of the copyright in this work and that any reproduction or use in any form or by any means whatsoever is prohibited without the written consent of UM having been first had and obtained;

(5) I am fully aware that if in the course of making this Work I have infringed any copyright whether intentionally or otherwise, I may be subject to legal action or any other action as may be determined by UM

Candidate's Signature: Date:

Subscribed and solemnly declared before,

Witness's Signature: Date:

Name:

Designation:

ABSTRACT

The aim of this work is to explore the possibility of combining boronizing and superplastic deformation on titanium alloy (Ti6Al4V) substrate. Superplastic boronizing (SPB) is carried out at three different temperatures of 1173 K, 1223 K, and 1273 K, and it is held for four different boronizing times of 1, 2, 3 and 6 hours. Titanium diboride (TiB_2) is the only boride compound identified after the boronizing process. Boronized layer thickness in the range of 44.9 to 149.3 μm is formed on the surface of Ti6Al4V and the surface hardness values increase with the respect of the formation's degree of the hard boronized layer. Diffusion coefficient values attained for all temperatures are 1.44×10^{-13}, 4.1×10^{-13} and 8.86×10^{-13} m^2s^{-1} respectively and the values are higher as compared to other works referred. The activation energy obtained for this process is 226.17 $kJmol^{-1}$. The results obtained suggest that the SPB process provides a more competent and efficient process for the formation of a boronized layer on the alloy.

ABSTRAK

Tujuan kajian ini adalah untuk mengenalpasti kemungkinan menggabungkan boronizing dan ubah bentuk superplastik pada aloi titanium (Ti6Al4V) substrat. Boronizing superplastik (SPB) dijalankan pada tiga suhu yang berbeza dari 1173 K, 1223 K dan 1273 K dan dijalankan selama masa berbeza-beza daripada 1, 2, 3 dan 6 jam. Titanium diboride (TiB_2) adalah satu-satunya sebatian boride dikenal pasti selepas proses boronizing itu. Ketebalan lapisan boronized dalam lingkungan 44.9 to 149.3 μm terbentuk di permukaan Ti6Al4V dan nilai kekerasan permukaan meningkat berkadar dengan tahap ketebalan lapisan boronized. Nilai kadar resapan diperolehi adalah 1.44×10^{-13}, 4.1×10^{-13} and 8.86×10^{-13} m^2s^{-1} dan nilai adalah lebih tinggi berbanding dengan kajian lain yang telah dijalankan. Tenaga pengaktifan diperolehi bagi proses ini adalah 226.17 kJ mol^{-1}. Keputusan yang diperolehi menunjukkan bahawa proses SPB ini menyediakan proses yang lebih cekap dan berkesan untuk pembentukan lapisan boronized pada aloi.

ACKNOWLEDGEMENTS

ALHAMDULILLAH, all praises to Almighty ALLAH s.w.t. Firstly, thanks to Allah s.w.t. for giving a good health and mind which enable me to complete this dissertation.

I would like to acknowledge my thanks to Dr. Iswadi Jauhari for his toughness to guide and teach me for the entire times of his supervision. I learned everything about research from him. Through his support and courage, I'm able to complete my research work successfully.

A special thanks to my beloved mother Puan Hjh. Shofiah binti Hamzah who always prays for my success and never fail to give me a full of supports from the first to the end. Also to all my family members, I'm very grateful for all of the sacrifices that you've made on my behalf. Your prayer for me was what sustained me thus far.

I would like to express my appreciation to the Superplastic's laboratory members who always walk along with me in this journey of research. I would also like to thank all of them for their help and support throughout my study.

Thanks also to Prof. Yukio Miyashita from Nagaoka University of Technology Japan for his kindness on giving many helps and advises during my stayed in his laboratory. I'm able to finish many of my research works and gained too much knowledge and experiences that are very meaningful to me.

I am indebted to all the technicians and staffs of the Department of Mechanical Engineering, University of Malaya and the Department of Mechanical Engineering, Nagaoka University of Technology, who helped and guided me with my works.

Nor Taibah Taazim

2016

TABLE OF CONTENTS

LIST OF FIGURES

LIST OF TABLES

CHAPTER 1 : INTRODUCTION

1.1 Background of Research

Titanium diboride (TiB_2) is well known for its excellent properties such as high hardness, high melting point, high elastic modulus and good wear resistance. Owing to these properties, it is mainly used for cutting tools, wear resistance and corrosion resistance part (Murthy et al., 2013).

Conventionally TiB_2 can be produced by a variety of processing methods, including the sintering, hot pressing, hot isostatic pressing, microwave sintering and dynamic compaction, in which the production cost for all of these methods is high. It is crucial to densify the TiB_2 since the boride has relatively low self diffusion coefficient due to the relatively strong covalent bonding of the constituents and also because of the oxygen rich layer (mainly TiO_2 and B_2O_3) that easily form on the surface of Titanium (Munro, 2000; Murthy et al., 2013; Zhao et al., 2014). A monolithic TiB_2 with 98% density has been successfully obtained through the sintering process at high temperature, 2750 K (2477 ^{0}C) and about 3 GPa of pressure is needed in order to compact the boride (Bhaumik, Divakar, Singh, & Upadhyaya, 2000).

Meanwhile, the TiB_2 coating formed by a pack boronizing process is recognized as well as inexpensive and not a very complex process. In this coating process, generally dual boride layer consists of titanium boride (TiB) and TiB_2 are formed. Though, it is desirable only to have TiB_2 layer since TiB is considered having much lower hardness (Atar, Kayali, & Cimenoglu, 2008; Li et al., 2010). Thus some of the boronizing techniques may produce only TiB_2, however the boride layer thickness is relatively thin (Atar et al., 2008; Tikekar, Ravi Chandran, & Sanders, 2007; Tsipas, Vázquez-Alcázar, Navas, & Gordo, 2010). The reason is because TiB_2 formation requires a high diffusion rate process. TiB_2 will only be formed after the boride grows to saturate. According to

the Ti-B phase diagram, the compound TiB_2 may exists at 30.1-31.1 wt% of boron compositions (Li et al., 2010; B. Sarma, Tikekar, & Ravi Chandran, 2012). The laser boriding is an example of a process that produced only the TiB_2 layer with the thickness layer in excess of 150 μm, without the formation of the TiB layer (Biplab Sarma, 2011).

Superplasticity has been applied in the surface hardening processes of metals, especially steels — under the tensile mode, initial pressure, compression mode and dual compression method conditions (Ahamad & Jauhari, 2012; Hasan, Jauhari, Ogiyama, & Ramdan, 2006; Jauhari, Yusof, & Saidan, 2011; Matsushita, 2011; Xu, Xi, & Gao, 1996). The initial pressure condition is considered the simplest method because it does not require extensive equipment to perform — only a simple specially designed clamp. Since the process involves the interaction between the solid powders and solid substrate, the principle of the initial pressure condition is almost similar to the diffusion bonding concept where during the initial stage of diffusion bonding, the asperities on each of the faying surfaces deform plastically as the pressure is applied and then followed by the creep and diffusion of atoms (Chaturvedi, 2011). For the metal substrate which has a fine grain size — less than 10 μm — the process could be accelerated by the superplastic deformation of substrate's surface asperities in the initial stage and the diffusion of atoms into fine grains in the following stage (Han, Zhang, Wang, & Zhang, 2005; Jauhari, Ogiyama, & Tsukuda, 2003; Xu et al., 1996). Thus, similar to the diffusion bonding, the initial pressure condition process is strongly dependent on the amount of the initial pressure applied, grain size and surface roughness of the metal substrate. Moreover the size of the powder is also an additional controlling parameter for the initial pressure condition (Azis, Jauhari, Masdek, Ahamad, & Ogiyama, 2010; Yusof, Jauhari, Rozali, & Hiroyuki, 2007).

Based on our previous study on superplastic boronizing (SPB) of duplex stainless steel through the initial compression method, a thick of boronized layer of about 46 μm has been successfully obtained by using a minimal amount of boron powder in a short period of time as compared to the conventional method (Hasan et al., 2006). The objective of this work is to explore the possibility of combining the boronizing and superplastic deformation on titanium alloy substrate. The behavior of the process is evaluated and the mechanism is determined in term of its activation energy value. The obtained results are expected to be very critical and useful for the applications of the boronizing in the industries.

1.2 Research Objectives

The objectives of this research are:

1. To study the feasibility of superplastic boronizing on Ti6Al4V and develop a uniform hard layer of TiB_2 using superplastic compression method.

2. To evaluate the properties of the boronized Ti6Al4V and the kinetic of superplastic boronizing on Ti6Al4V.

1.3 Outline of Research

The outline of this dissertation is divided into five chapters which are elaborated as follows:

Chapter 1: The introduction briefly describes the overview of the titanium diboride (TiB_2) including the properties, commercial production method, and the related problem statement. It reviews and compares the previous studies regarding the superplastic methods and provides the importance of parameters that give a direction to this research work. The objectives of this study are presented followed by the research methodology. The dissertation outline is given at the end of the chapter.

Chapter 2: Literature Review is mainly based on the theories and summaries of superplasticity, boronizing, superplastic boronizing, TiB_2 and some other allied topics. It reviews from the various sources such as journals, text books, previous dissertations reports, and the world wide webs.

Chapter 3: Experimental Procedure is divided into three stages. This involved: (I) the preparation of developing the boronizing process, (II) the boronizing process, and (III) collecting and analysing of data. This section depicts the details on each of the procedures. Some of the characterization techniques such as scanning electron microscopy (SEM), X-Ray diffraction analysis and Vickers hardness measurement are also described in this chapter.

Chapter 4: Results and Discussions examine and discuss all the results obtained from the X-Ray diffraction analysis, boronized thickness measurement, microstructure evaluation and hardness testing. It also includes the calculation for determining the

kinetics of the superplastic boronizing process. This section compares the results obtained with other works reported.

Chapter 5: Conclusions and Recommendations summarize all the obtained results. The possible future works that can be conducted are also recommended in this chapter.

CHAPTER 2 : LITERATURE REVIEW

2.1 Superplasticity

Superplasticity is defined as the ability of polycrystalline materials to exhibit in a generally isotropic manner, very high elongations prior to failure. In general, superplasticity can be defined as a phenomenon of materials that are able to undergo a large uniform strain prior to failure in excess of 200% or more. As reported by Higashi, the current world record for elongations in metals stands at 8000% elongation in commercial bronze. Figure 2.1 demonstrates the superplasticity in Cu-Al alloy at 8000% of elongation during a tensile test. SP does not refers to a class of materials, but connotes the deformation characteristics of any given material under a narrow range of temperature and rate of loading (Chandra, 2002; Tsuzuku, Takahashi, & Sakamoto, 1991).

Figure 2.1 : **Superplasticity in Cu-Al alloy (8000% elongation) (Russell & Lee, 2005).**

2.1.1 Characteristics of Superplasticity

It has been reported that superplastic behavior in most metals, alloys and ceramics are associated with three main characteristic: (a) a fine grain size (on the order of 1-10 μm), (b) deformation temperature > 0.5 T_m (where T_m is the absolute melting point) and (c) a strain rate sensitivity factor *m* which is more than 0.3 (Hertzberg, 1996).

a) Strain rate sensitivity

A high strain rate sensitivity of flow stress (m) is the most important mechanical characteristic of a superplastic and it is defined as follows:

$$\sigma = k\, \dot{\varepsilon}^{m} \qquad (2.1)$$

where σ is the flow stress and ε̇ is the strain rate. The elongation to failure in tensile specimen of superplastic material increases with increasing value of m. In fine-grained superplastic materials, m value is about 0.5 (Chakrabarty, 2010).

b) Fine grain size

Fine grain is one of the main characteristic of superplasticity. The ductility of material increases as the grain size become finer. It is critical for the material to have a fine grain structure in order to create a superplasticity in a material or to deform a material in the superplastic condition. Metals are not normally superplastic unless their microstructure is a fine grain typically 1-10 μm in diameter and the structure must also be stable at temperature of deformation (H.A.M. Yusof, 2010). The fine grain microstructure is important because the presence of many grain boundaries acted as a short circuit paths for diffusion (Han et al., 2005).

c) High Temperature

Superplastic deformation and the movement of matter are affected by the temperature. Superplasticity in most materials commonly occurs at an elevated temperature ($T > 0.5\ Tm$). At these temperature there is equilibrium between the recovery and hardening, so that the metal does not strain hardening (H.A.M. Yusof, 2010) and the grain boundary sliding is noticed to be active and the deformation can be classified as “superplastic”. It

is noted that SP deformation is active but influenced by a dynamic recrystallization and dynamic grain growth (Vanderhasten, Rabet, & Verlinden, 2005). Figure 2.2 shows the relation betweenσ, ἑ, m, effect of grain size and temperature on superplasticity.

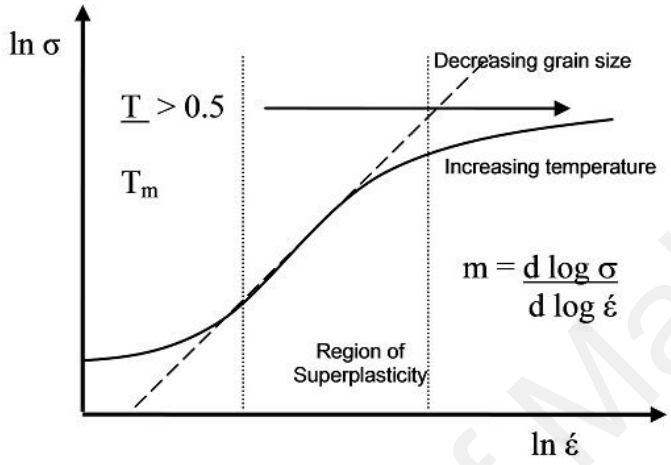

Figure 2.2 : Normalized curve of log stress versus log strain.

2.1.2 Mechanism of superplasticy

Until todays, the exact mechanism of superplasticity is still not yet completely understood. Several models of mechanisms have been proposed for the superplastic deformation (Gifkins, 1976; Langdon, 1970; Mukherjee, 1971; Rosen, Arieli, & Mukherjee, 1980). Recent studies using the high voltage transmission electron microscope support the idea that the grain boundary sliding is the primary mechanism. Figure 2.3 explains the evolution of microstructure and texture during superplastic deformation. However during the superplastic deformation, strain in a given direction is due to the motion of individual grains or clusters of grains relative to each other by sliding and rolling. Grains are observed to change their neighbours and seen to emerge at the free surface from the interior. During deformation, the grains remain equiaxed or

become equiaxed. Texture an indicator of the volume of grains in a given spatial orientation decreases in intensity with superplastic flow.

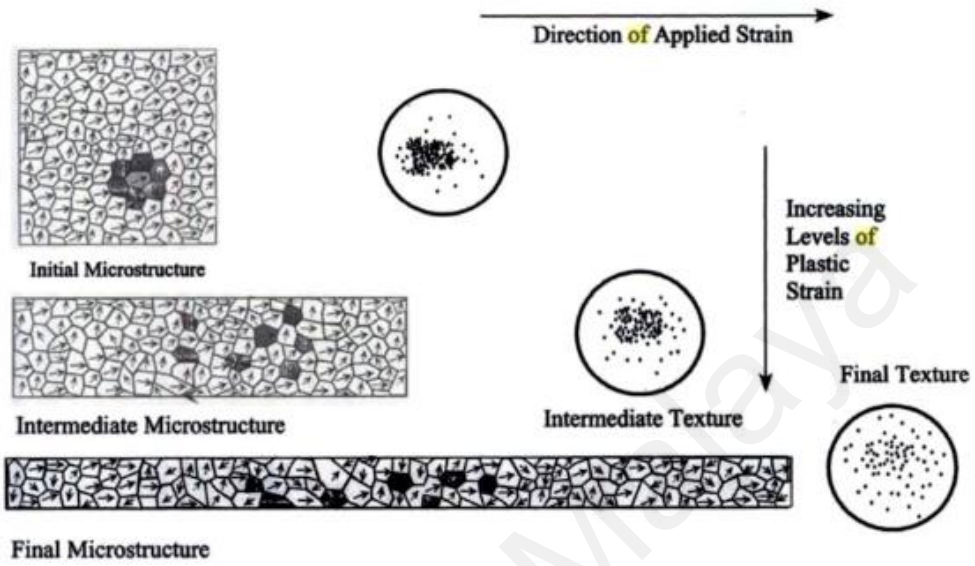

Figure 2.3 : Evolution of microstructure and texture during superplastic deformation (Totten, Funatani, & Xie, 2004).

During the process of the diffusion accommodation, the mass flow is due to the diffusion process at the vicinity of grain boundary. When a load is given to a material, the deformation is due to the grain boundary diffusion and sliding, as a result of strain (Figure 2.4 (a)).

While for the accommodation by a dislocation motion, it can be understood by dividing the grain into two path; the core inside the grain, and the mantel at the grain boundary (Figure 2.4 (b)). In order for the grain to slide, the dislocations which move onto the grain boundary are accumulating at the triple point of grain boundary. From there, the dislocation move into the mantel due to the stress concentration. Thus the dislocation motion inside the mantle results in the grain rotation. Figure 2.4 (c) shows the process

of accommodation by dislocation motion and Figure 2.4 (d) shows the model that suggests a rotation of grains in addition to sliding.

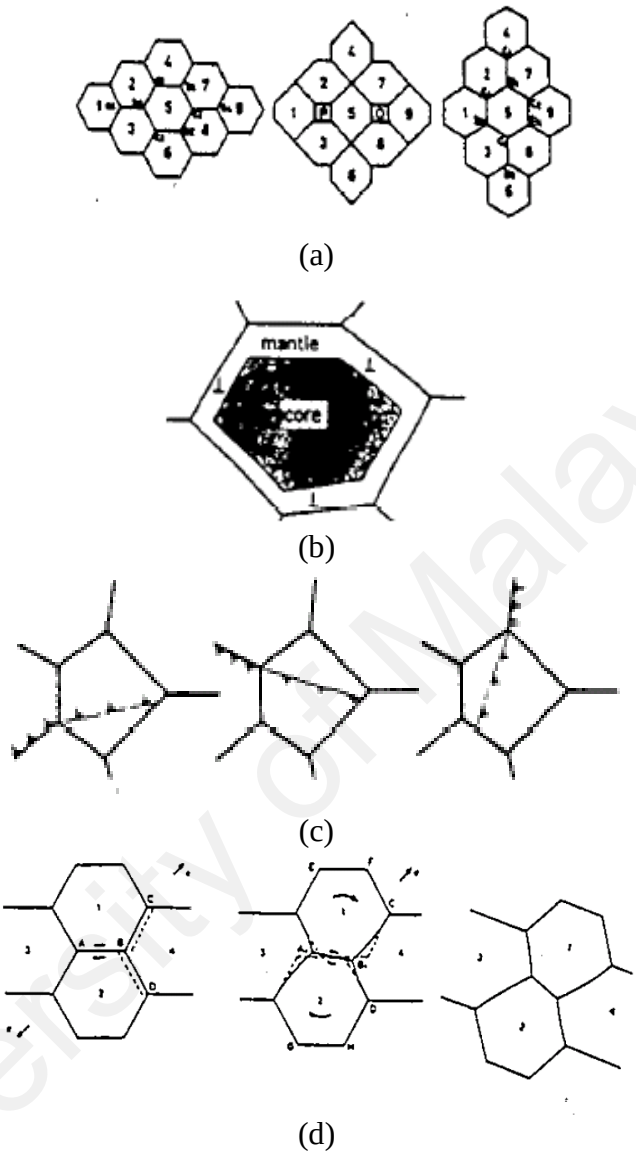

(a)

(b)

(c)

(d)

Figure 2.4 : Basic accommodation mechanism of superplasticity (a) diffusional accommodation (b) deformation in mantle of grain (c) dislocation motion inside the mantle result in the grain rotation (d) Model suggests of rotation of grains in addition to sliding (Zelin & Mukherjee, 1996).

2.1.3 Application of Superplasticity

Superplasticity has been developed and implemented on several application processes. There are two major processes in using superplasticity for commercial applications. The first is the superplastic forming (SPF) which utilizes large deformability of the superplastic material and the other one is the superplastic diffusion bonding (SPDB) where a good bonding is achieved on the bonding interface as a result of local superplastic flow (Kum, Oyama, Sherby, Ruano, & Wadsworth, 1984).

Superplasticity is mostly being used to form parts in the aerospace application (Tsuzuku et al., 1991; Wang & Zhang, 1988) even though nowadays there are also found used in some other non-aerospace application. In the aerospace application, this superplastic forming is increasingly being used to form a very complex geometry. Nickel-base alloys are used to form a turbine discs with integral blades while aluminium alloys are fabricated to form a low weight and high stiffness airframe control.

2.1.3.1 Superplastic Forming (SPF)

Superplastic forming is usually conducted under a high temperature and also controlled the strain rate. This process is typically obtained by a single-sided die where the sheet is heated at a high temperature and gas pressure applied in order to push the sheet into the tool (Friedman & Luckey, 2004). Figure 2.5 shows the illustration of the SPF process.

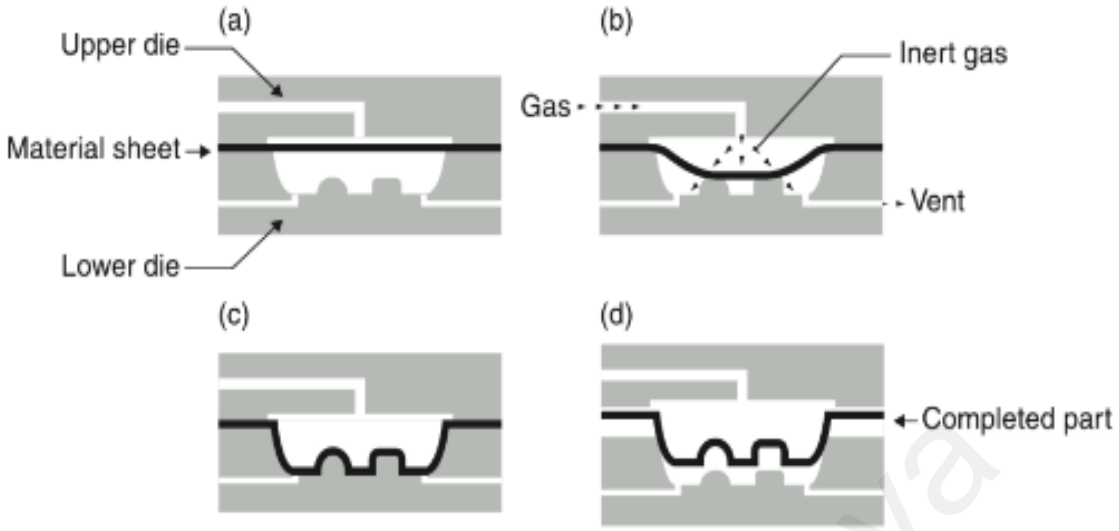

Figure 2.5 : Single sheet blow forming of SPF materials showing the cross-section of die and sheet: (a) initial flat sheet inserted in between upper and lower dies; (b) progression of forming under gas pressure; (c) final shaped part in contact with lower die; and (d) removal of the part (Giuliano, 2011).

Due to the normal low die costs and relatively slow forming rates, this process is usually found to be economically viable from a small to the moderate production quantities (Bloor, Brook, Flemings, & Mahajan, 1994), as a fact that only a single configuration die is used. Moreover, it is also suitable to permit a short lead time to produce the part once the design is completed.

2.1.3.2 Solid State Diffusion Bonding (DB)

Superplasticity also plays an important role in the solid state diffusion bonding (DB) process. It was reported that the superplastic deformation accelerates the solid state diffusion bonding process while obtaining an effective bonding (high strength) with a minimum material deformation (Jauhari et al., 2003). The acceleration of solid state joining by superplastic deformation is closely related with the development of grain

boundary sliding in the material (Lutfullin, 1995). This process permits fabrication of parts with local thickness variation, attachments and complex sandwich structure (Bloor et al., 1994). SPF together with DB has been implemented to produce the hollow engine blades, fan and compressor blades for aero engines (Xing, Wang, Zhang, & Wang, 2004; Xun & Tan, 2000). The superplastic diffusion bonding (SDB) is often combined with the superplastic forming (SPF) in the manufacture of complex cellular structures. Compared to the other diffusion bonding processes, the SDB process offers a shorter joining time at a lower pressure, with parent metal strength (Jauhari et al., 2003).

Figure 2.6 shows the Schematic illustration of superplastic diffusion bonding process. During the diffusion bonding process, at a elevated temperature, a two clean of a metallic surfaces are brought into contact under some amount of pressure. The two surfaces are far from smooth on the atomic scale and consist of asperities and voids in point to point contact. Besides, the contact point between the two surfaces comprises a small fraction of the total surface area. On the application of the pressure, the contact area is expanding in order to support that pressure − in other word, the two contact surfaces undergo deformation process. The voids in the bond interface are filled by a two processes: a time dependent plastic collapse by a superplastic flow and a diffusive mass transfer, in which it involves a grain boundary diffusion and volume diffusion from the bond interface to the surface of the voids. After a full contact, the bond interface disappears by a subsequent diffusion between the two contact areas (Hanliang Zhu, 2005).

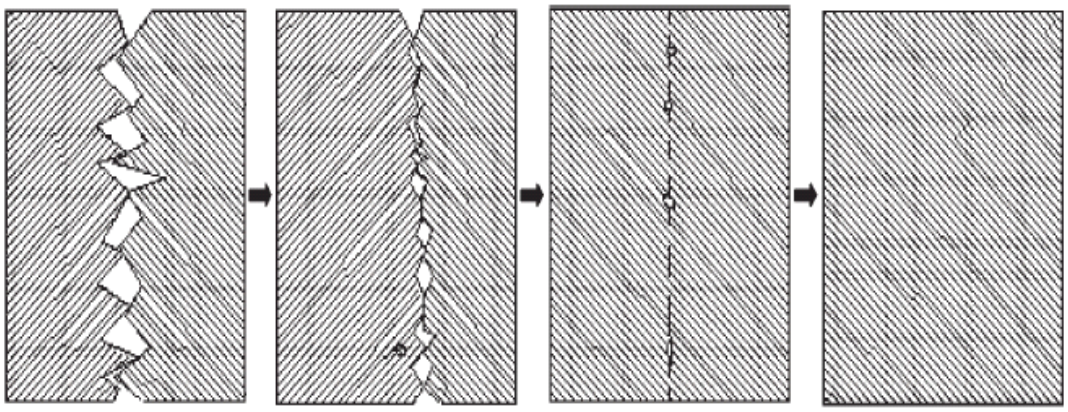

Figure 2.6 : Schematic illustration of superplastic diffusion bonding process.

2.2 Boronizing

Boronizing is a thermo-chemical surface treatment process which involving in the atom diffusion on the surface of the substrate material to form a boride layer that give the high surface hardness of the material. The diffusion hardening or strengthening of material is a method of an increased resistance to the deformation. The movement of dislocation in the metal facilitates metal deformation (Conway, 2006). Therefore the presence of solute atoms (boron) in the solvent (titanium matrix) phase lattice distort the latter, thereby may causing a local stress fields that act as the barriers to the mobility of the dislocation and thus strengthen the metal (Shangguan, 2005).

Boronizing typically requires the process temperature of 973K to 1273K in either gas, solid, or liquid media (Genel, Ozbek, & Bindal, 2003; Yapar, 2004). The thickness of boride layer formed is determined by the temperature and time of the treatment (Jain & Sundararajan, 2002).

2.2.1 Conventional boronizing

The medium for the boronizing process can be either in gaseous, liquid or solid form. Therefore the development work has been carried out in all three fields. Since the gas offers a number of distinct technical advantages as a diffusion medium, it has been used successfully, for example, for case hardening, nitriding and carburizing.

In addition, the powder pack boronizing process is a simple, economical, original and industrially reliable (Driver, 1981). In this process, the work piece is placed in a suitable container and embedded in the boronizing agent, which then activated the boron carbide. In order to minimize the consumption of the latter, the container and work piece should be placed at the same shape. To avoid the complications, the boronizing process should be performed in a protective gas atmosphere, which may be either a nitrogen or pure argon; or a mixture of hydrogen and either nitrogen or argon. This is accomplished either by packing the containers into a protective gas retort and heat-treating them in a chamber furnace, or else boronizing directly in a retort furnace with the necessary protective gas supply (Hasan, 2006).

2.2.2 Superplastic boronizing

The process which involves the combination of both, the superplastic deformation and boronizing is called the superplastic boronizing process. The basic principle of superplastic boronizing process is to conduct the boronizing where the specimen will be undergoing into the superplastic deformation (Xu *et al*, 1997).

From the previous work on the superplastic boronizing, the process was conducted through a tension loading method. A tensile specimen was pulled in contact with the solid boronizing agents on a tensile test machine. During the superplastic boronizing,

the superplastic deformation created a high density of vacancies, dislocations, and sub-grain boundaries. These defects are movable under the superplastic deformation − boron atoms will diffuse into the vacancies in the grain and at the grain boundary side hence increase the rate of atomic diffusion. (Xu, Xi, & Gao, 1997).

Xu *et* al. 1997 has reported that this process has a much faster boronizing rate compared to the conventional boronizing method, and also produces the boronized layers with better mechanical properties.

In the same work, Xu *et* al. had found that the results indicate that superplastic boronizing has improved the fracture strength of the specimens by 8%, the toughness by 18% and the maximum flexure by 1%. Compared to the conventional boronizing, the borides grains produced by superplastic boronizing are smaller and non acicular. When the cracks growth along or cross the borides grains, they constantly meet a new grains. Consequently, the cracks have to change their propagation directions, which consumes energy and slow down the propagation speed of the cracks. All these factors reduce the brittleness and improve the mechanical properties of the boride layers which are produced by the superplastic boronizing. It is believed that the microstructural and micro-compositional changes are affected by the mechanical-property improvement.

Meanwhile, for the superplastic boronizing process through dual compression method, an external force had been applied to the compressed surface. The apparatus setup for this process is shown in the Figure 2.7 below.

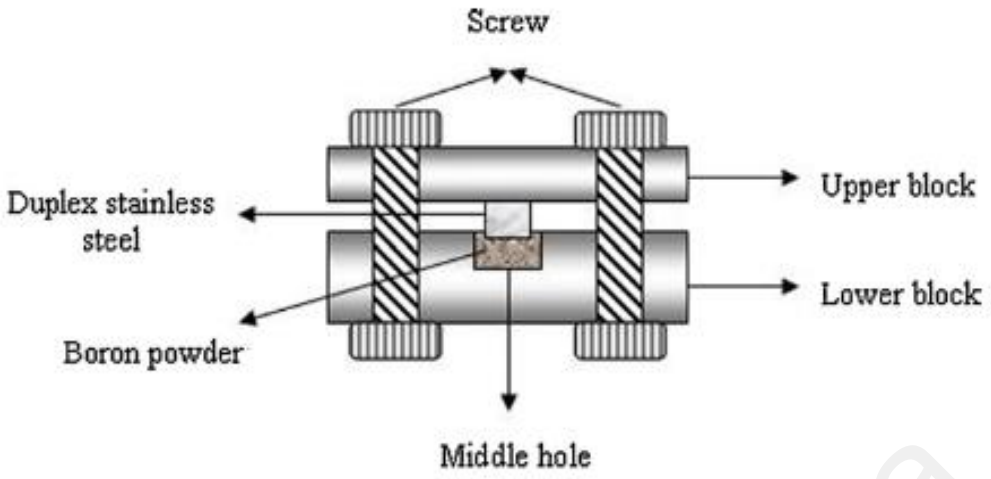

Figure 2.7 : Schematic diagram of clamp (Jauhari et al., 2011).

The application of the external force is to compact the boron atoms so that the interaction areas between the atoms and the substrate can be increased. It was understood that during the early stages of the solid state diffusion bonding process, the asperities on each of the faying surfaces deform plastically as the pressure is applied. The fine grain microstructure of the superplastic materials would also accelerate the following stages. Through the superplastic deformation, the movement of atoms into the specimen was highly accelerated by the grain boundary sliding process leading to the formation of thick boronized layer in an extraordinarily short period of time (H. A. M. Yusof, 2010).

There are a few factors that are affecting the rate of the superplastic boronizing process. It is similar to the diffusion bonding, the initial pressure condition process is strongly dependent on the amount of the initial pressure applied, grain size and surface roughness of the metal substrate. Moreover the size of the powder is also an additional controlling parameter for the initial pressure condition. Figure 2.8 shows an illustration of boronizing process for a different (a) surface roughness and (b) boron powder

particles size condition. These are the examples of the factor that are controlling the parameter for the initial pressure condition. As can be seen from the Figure 2.8 (a) the surface of the substrate is rough subsequently the distance between the powder particles and the surface is large and vise versa. It also can be seen from the Figure 2.8 (b) the size of the boron particle is big then the contact area between the boron particles and the surface of substrate is small and vise versa. These two factors influence the rate of the diffusion process. This is because as the distance and the contact area between the boron particles and the surface is shorter and larger respectively, the diffusion of boron atoms into the substrate could be accelerated (Azis et al., 2010; Yusof et al., 2007).

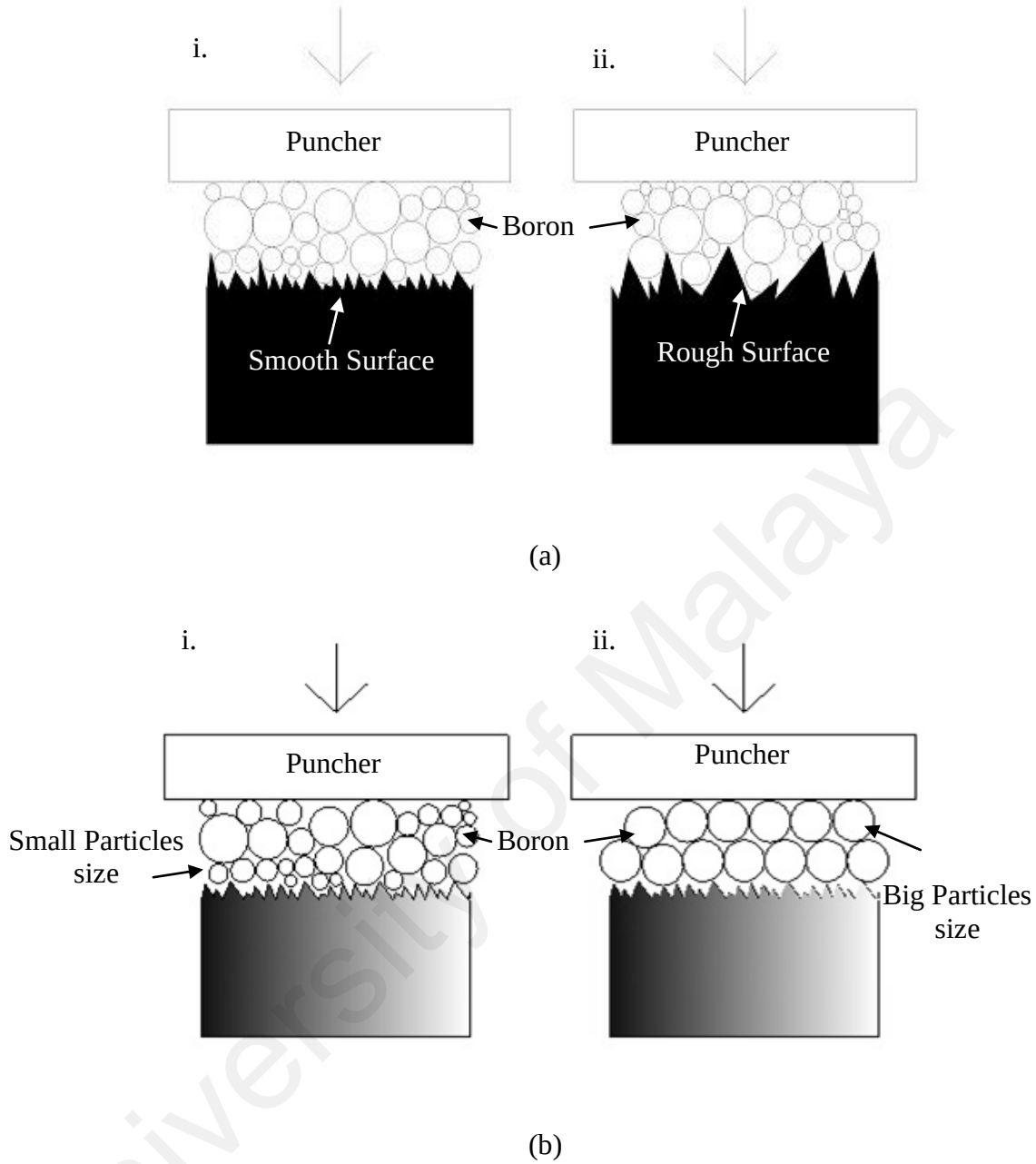

Figure 2.8 : Illustration of boronizing process (a) for a different surface roughness and (b) boron powder particles size condition.

2.3 Material

2.3.1 Titanium and Titanium Alloy

Titanium and its alloy are an attractive material since they have a high strength-to-weight ratio, where the elevated temperature properties used as high as about to 550ºC, and is excellent in the corrosion resistance, particularly in the oxidizing acids and the chloride media and in most of the natural environment. The high strength-to-weight ratio and the high elevated-temperature properties of titanium alloys are the prime importance stages in the aerospace industry.

The metallurgy of titanium is dominated by the crystallographic transformation which takes place in the pure metal at the temperature of 882°C. Below this temperature, pure titanium has a hexagonal close packed structure known as alpha (α); while above the temperature, the structure is body cantered cubic and termed as beta (β). The control of α and β phase through the alloying element addition is the basis part for titanium being used by the industry today. There are 2 types of alloying element in which are known as α stabilized System and β stabilized System (*Internet reference*). This titanium alloy can be classified into three main groups as follows: (1) Alpha alloys (2) Alpha-Beta alloys (3) Beta alloys (*internet reference*).

Ti6Al4V is an Alpha-Beta alloys, with 6 wt% aluminium stabilizing the α phase and 4 wt% vanadium stabilizing the β phase. At a room temperature the microstructure at equilibrium consists mainly of the α phase (hcp) with some retained β phase (bcc). The microstructure depends on the cooling rate and the prior heat treatment. It is divided into several types, namely as grain boundary allotriomorph α, global or primary α (called bi-modal microstructure when the globular α is surrounded by Widmanstatten platelets). Widmanstatten, basketweave, and martensitic. A recently described

microstructure is the bi-lamellar, in which the retained β phase lying between in the α platelets in a Widmanstatten structure, itself contains thinner secondary α platelets (Lütjering, 1998).

Ti6Al4V is the most important and widely used among the other titanium alloy and they have the greatest commercial important, making up more than half the sales of the titanium alloy both in Europe and United States. The offer on the prospect is relatively high tensile strength and in good formability, despite of some sacrifice in creep strength occurs above the 400ºC as well as when the weldability is reduced (Polmear, 1981).

2.3.2 Superplasticity of Ti 6Al 4V

While not all the materials exhibit the superplasticity, a wide range of materials including metals, ceramics, metallic/intermetallic/ceramics matrix composites, intermetallics and nanocrystalline materials show this behaviour at some special loading conditions. Most of these materials require some special processing conditions to achieve the necessary of microstructural requirements for SP. However, some materials which is commercially processed exhibit the superplastic behavior, e.g. Ti6Al4V alloy (an aerospace workhorse material) (Chandra, 2002). Ti6Al4V are well known for their potential as the superplastic materials because the microstructure is composed by the two crystal structures of α and β structure.

Regarding to the schematic phase diagram of Ti6Al4V (Figure 2.9) at a room temperature, the microstructure is mainly composed of hexagonal close-packed structure (α) phase and a little of body-centre cubic (β)-phase. Above the 600ºC, α phase undergoes an allotropic transformation to β-phase, while above 996ºC (beta transus

temperature) the whole microstructure is composed of equiaxed β grain (Polmear, 1981).

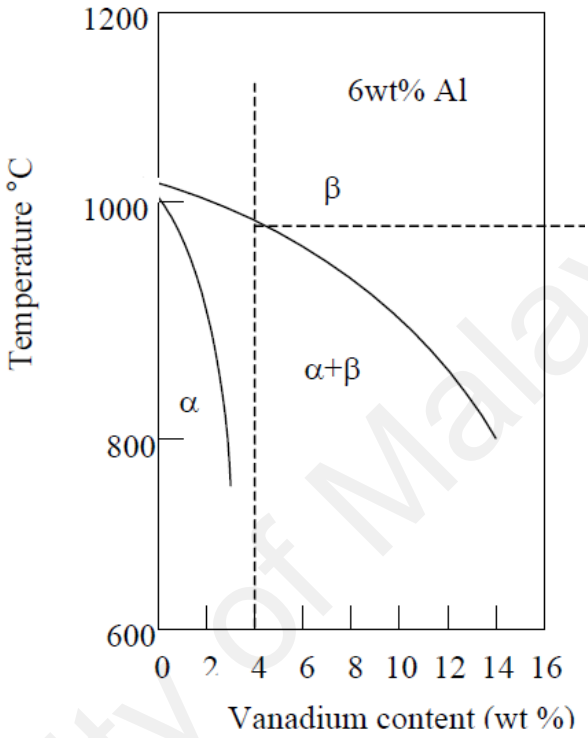

Figure 2.9 : Phase Diagram of Ti 6Al 4V.

2.4 Titanium diboride (TiB_2)

Titanium diboride (TiB_2) is a ceramic material and is well known for its excellent properties such as high hardness, high melting point, high elastic modulus and good wear resistance. Owing to these properties, it is mainly used for cutting tools, wear resistance and corrosion resistance part (Murthy et al., 2013).

Conventionally TiB_2 can be produced by a variety of processing methods, including the sintering, hot pressing, hot isostatic pressing, microwave sintering, and dynamic compaction in which the production cost is high. It is crucial to densified the TiB_2 since

the boride has relatively low self diffusion coefficient due to the relatively strong covalent bonding of the constituents and also because of the oxygen rich layer (mainly TiO_2 and B_2O_3) that easily form on the surface of Titanium (Munro, 2000; Murthy et al., 2013; Zhao et al., 2014). A monolithic TiB_2 with 98% density has been successfully obtained through the sintering process at high temperature (2750 K) and about 3 GPa of pressure is needed in order to compact the boride (Bhaumik et al., 2000).

Meanwhile, the TiB_2 coating formed by a pack boronizing process is recognized as well as cheap and not a very complex process. In this coating process, generally dual boride layer consists of TiB and TiB_2 are formed. TiB_2 will only be formed after the boride grows to saturation. According to the Ti-B phase diagram, the compound TiB_2 may exists at 30.1-31.1 wt% of boron compositions as shown in Figure 2.10 (Li et al., 2010; Murray, Liao, & Spear, 1986; B. Sarma et al., 2012).

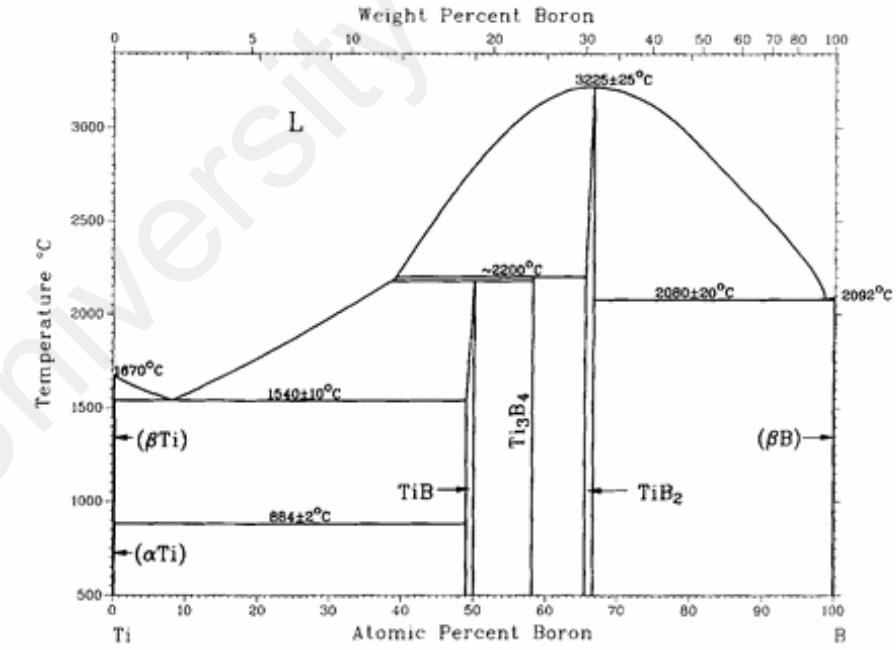

Figure 2.10 : Ti-B phase diagram.

2.5 Kirkendall Effect

When we consider a binary solution of A and B, the rate at which A and B diffuse are not necessarily equal. It is observed that, usually the lower melting component diffuses much faster than the other. This lead to certain effect which are interesting and observed by Kirkendall (Munro, 2000).

The Kirkendall effect can be described by the motion of the boundary between two metals due to a thermally activated and unbalanced diffusion rate of the constituents. For instance, upon annealing of two stacked metals, A and B, at a sufficient temperature to thermally activate the diffusion of atoms, atomic migration can occur at the interface where atoms diffuse from metal A to metal B and vice versa (Figure 2.11 and Figure 2.12). According to the Kirkendall effect, the position of the initial interface changes during the annealing process since the atomic diffusion coefficients of atom A in metal B and of atom B in metal A are different. As a consequence of the unbalanced diffusion rates between the two stacked metals, vacancies will be injected at the interface region within the faster diffusing metal (El Mel, Nakamura, & Bittencourt, 2015).

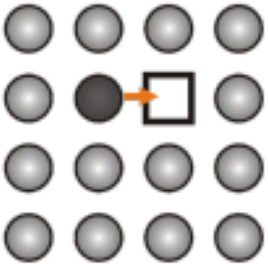

Figure 2.11 : The mechanism of the atomic diffusion process by a vacancy mechanism (El Mel et al., 2015).

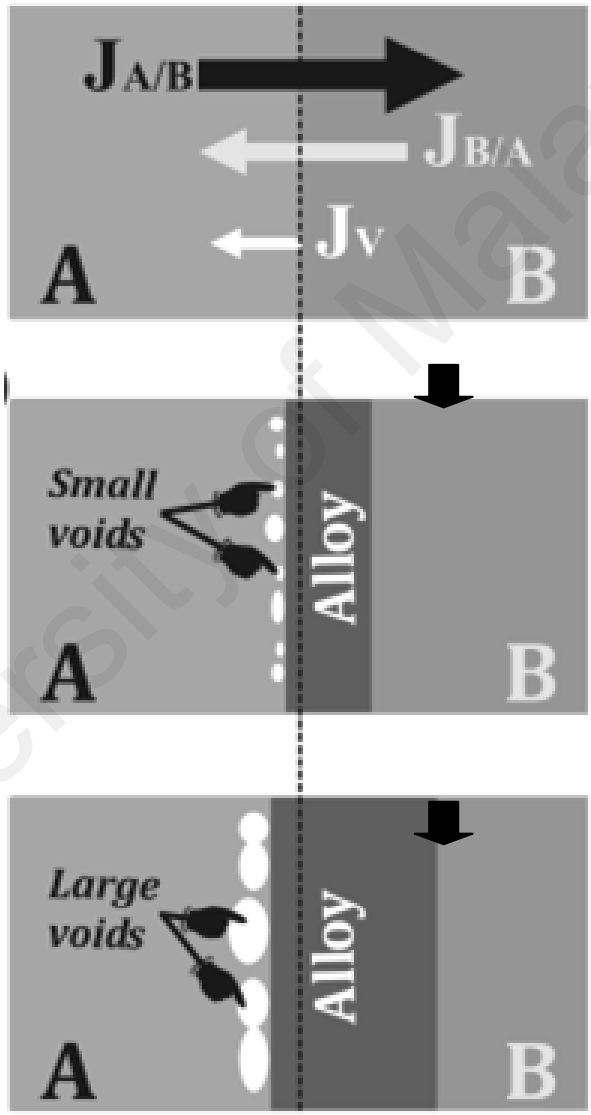

Figure 2.12 : Schematic illustration describing the different stages occur during the formation of voids at the interface of voids at the interfaces of two different metals A, and B, as a consequence of the Kirkendall effect induced by thermal thermal annealing (El Mel et al., 2015).

CHAPTER 3：EXPERIMENTAL PROCEDURE

3.1 Substrate material

A commercial grade of Ti6Al4V is used as the substrate material. Table 3.1 shows the chemical composition of the substrate. The specimens are cut into a dimension of 10 mm x 4 mm x 3 mm using a diamond cutter machine. Figure 3.1 shows the image of as received specimen.

Table 3.1 : Chemical composition of Ti6Al4V.

Element	Titanium (Ti)	Aluminum (Al)	Vanadium (V)	Carbon (C)
wt %	88.05	6.73	3.90	2.12

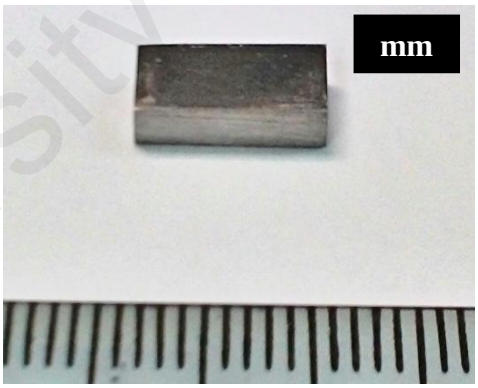

Figure 3.1 : Image of as-received specimen.

3.2 Grinding and Polishing

Prior to boronizing, the specimen surfaces are ground using an emery paper to remove the oxide layers and irregularities. The emery paper with grade of 100, 240, 400, 600, 800, 1000, 1200, 1500 and 2000 are used for the grinding process. It is started from the coarse to the finest grade. After the grinding process is completed, the specimen is cleaned with an alcohol to remove contaminant.

The polishing process is done to achieve a high reflective surface of specimen with free scratch. The specimen's surface is polished by using a polishing cloth until a mirror like surface is obtained. The average surface roughness (Ra) of the surface to be boronized is 0.01 μm.

3.3 Boron Powder Preparation

Commercial Ekabor-1 powder by Bortec Germany is used as a boronizing agent. Figure 3.2 shows the image of boron powder. Initially the particle size of the boronizing powder is less than 150 μm. However, this size is considered very big for the boronizing process. Therefore, the powder is ground to a smaller particle size by using a ball mill for a few hours. Then it is sieved by using a stainless steel sieve tool. The sieving process is started from the biggest to the smallest sieve opening. Boron powder with particle sizes of less than 45 μm is used for this experiment. Figure 3.3 shows an illustration of the sieving process.

Figure 3.2 : Image of boron powder.

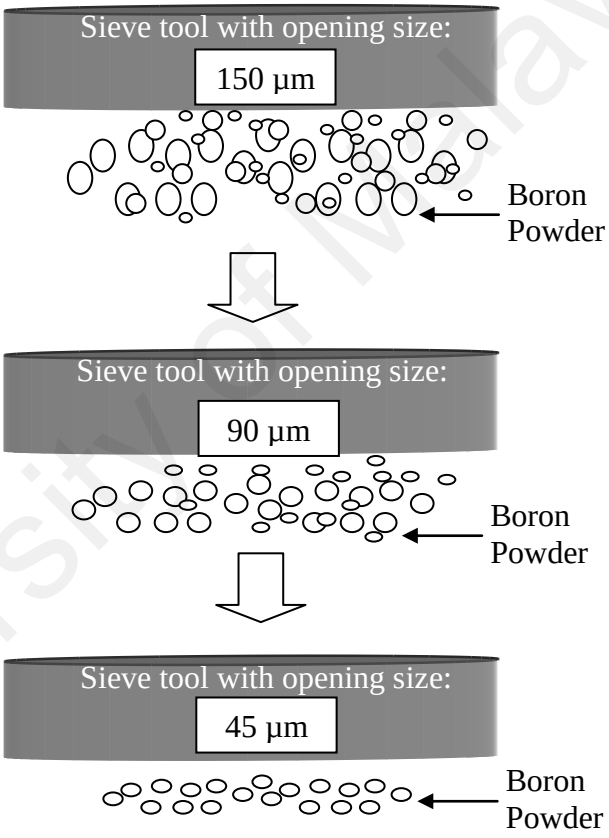

Figure 3.3 : Illustration of the sieving process.

3.4 Design and fabrication of clamp

For SPB, a special clamp is used. The clamp has an upper block, a lower block, hole, puncher and two parts for a screw. The specimen is placed and covered with the boron powders in the middle hole of the lower block. The upper block and the puncher are attached together and both are paired up with the lower block. Function of puncher is to compress the samples and compact the powder hence increase the interaction area between powders and samples. The initial pressure is applied by tightening the screws and nuts using a torque wrench. Figure 3.4 shows the schematic diagram of the clamp.

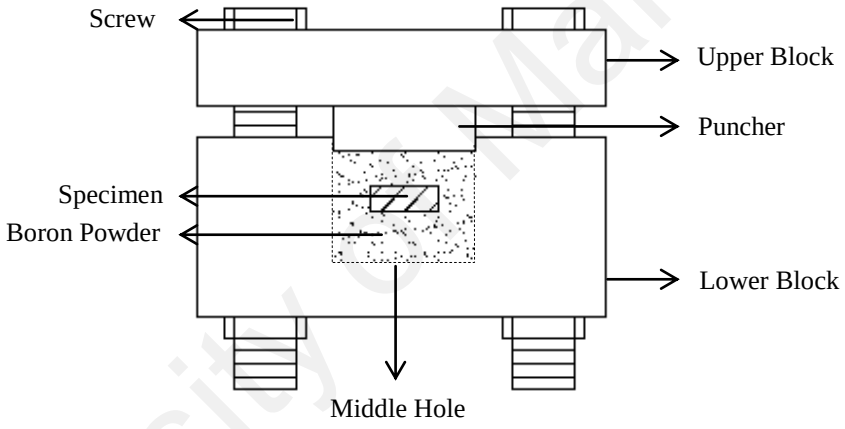

Figure 3.4 : Schematic diagram of clamp for SPB.

In addition, the clamp needs a holder to hold it in the furnace. This holder ensures the clamp to be placed at the centre of the chamber. Figure 3.5 shows the schematic diagram of the clamp with the holder. The material which been used for the clamp and holder is stainless steel SUS 304. This material is suitable for a high operating temperature application. The fabrication process of the clamp involves cutting, milling, phrasing, and drilling. Figure 3.6 to 3.8 show the detail drawing of the clamp and holder for the fabrication process.

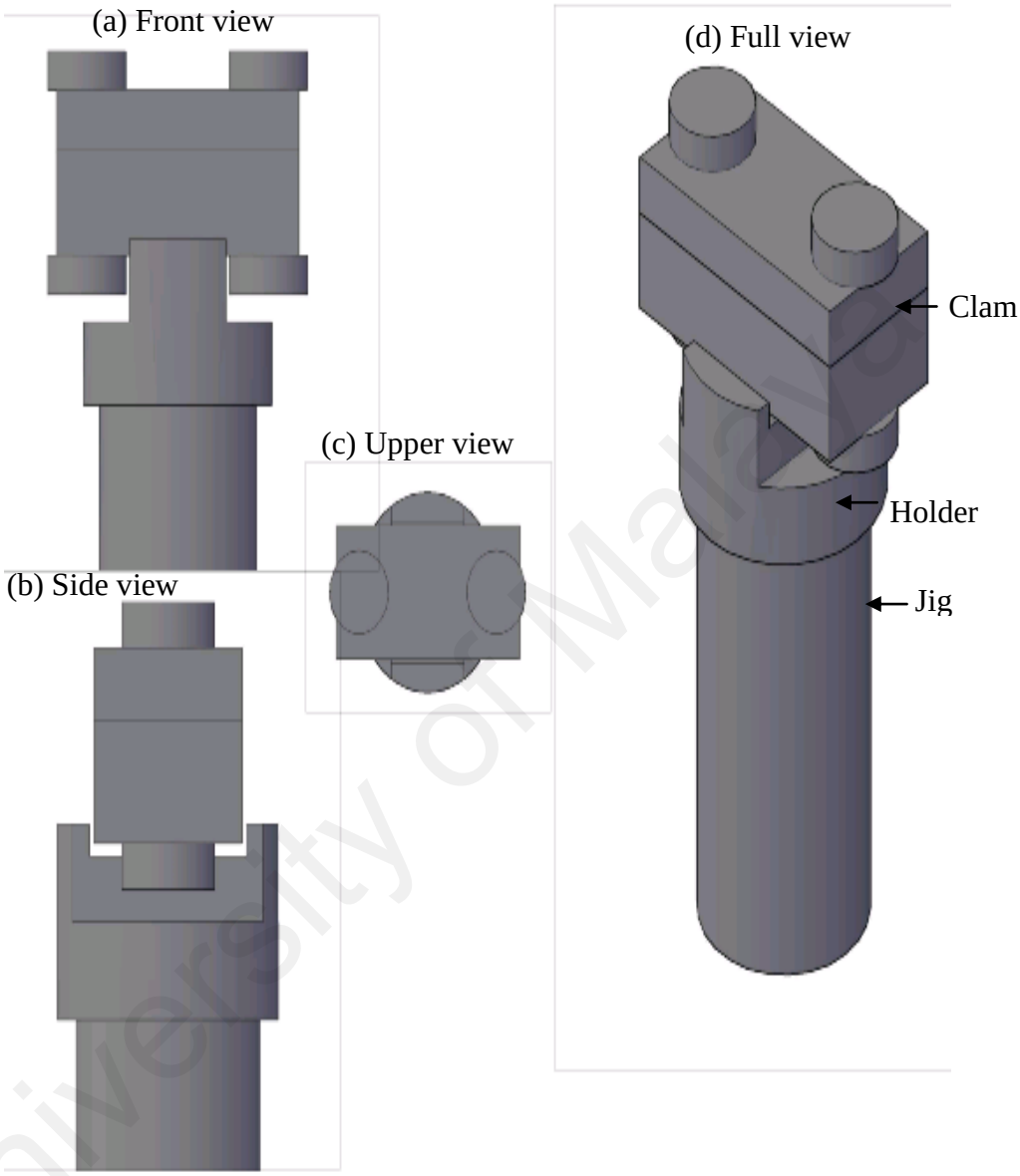

Figure 3.5 : The schematic diagram of the clamp with the holder.

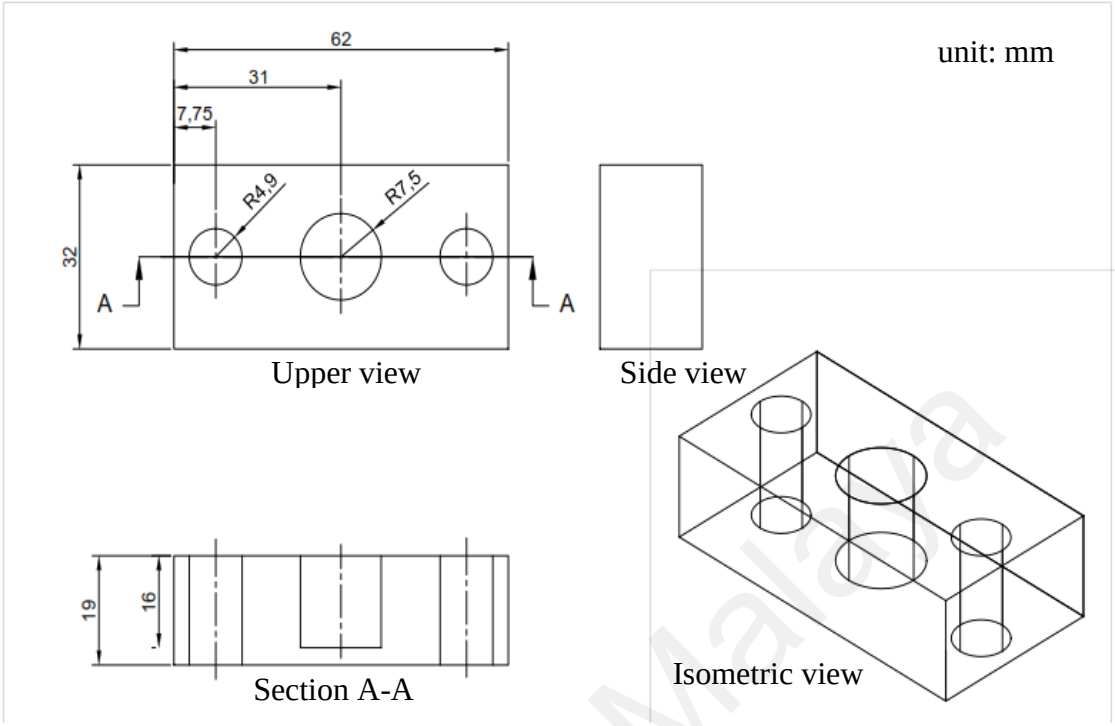

Figure 3.6 : Drawing of the lower block of clamp.

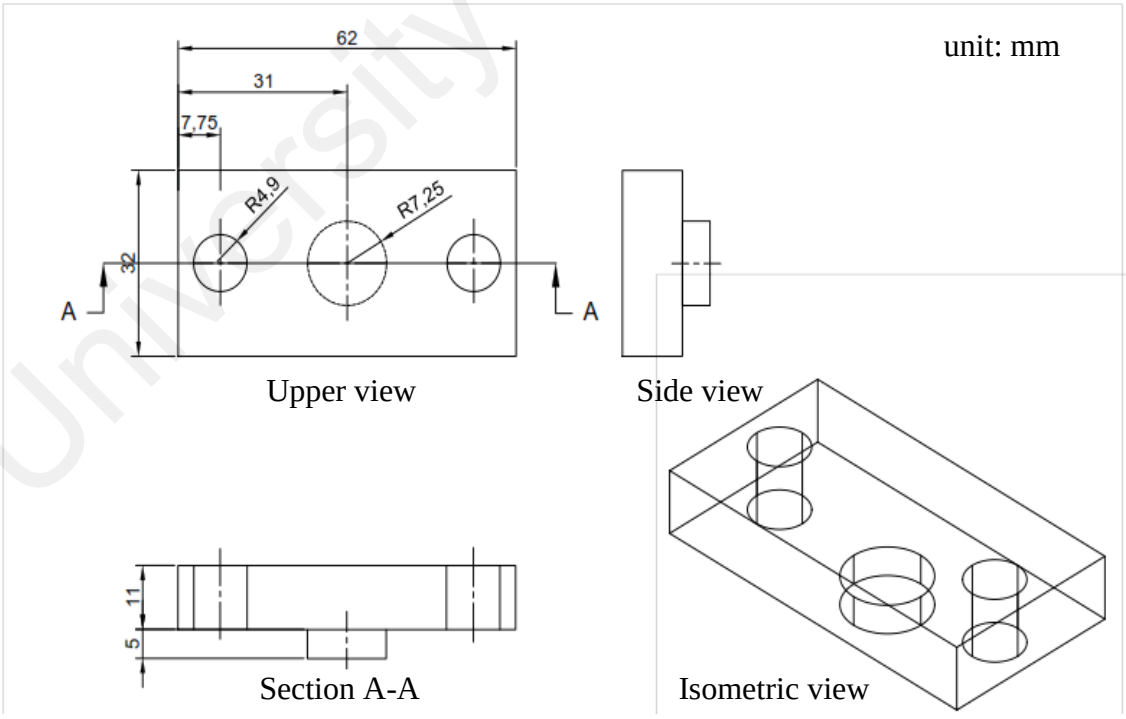

Figure 3.7 : Drawing of the upper block of clamp.

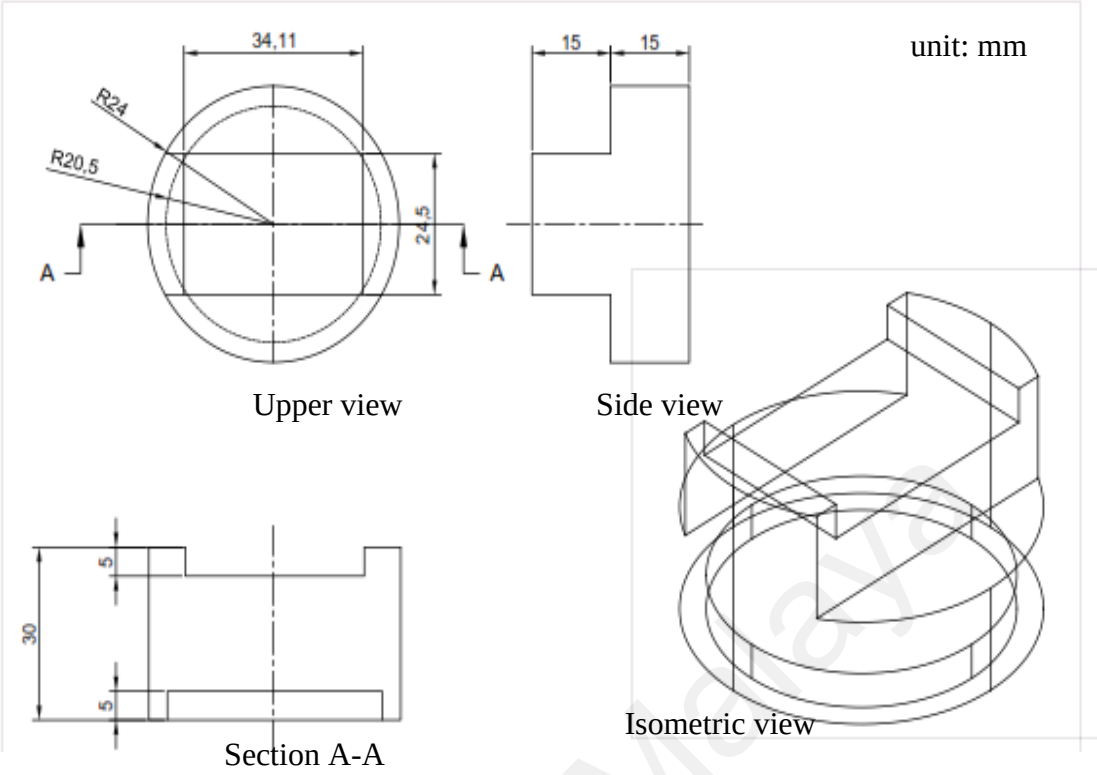

Figure 3.8 : Drawing of the clamp's holder.

3.5 Boronizing Process

In the SPB process, a special clamp is designed and fabricated. The boron powder is filled inside the middle hole of the clamp and the initial pressure of about 333 MPa is applied by tightening the clamp screws and nuts using a torque wrench.

The yield strength of the titanium alloy at an ambient temperature is about 895 MPa (Natali, 2003) . The initial pressure of 333 MPa is chosen because it is about 30% of the yield strength thus would not be able to cause a plastic deformation to the bulk of the substrate, but could give enough pressure for the plastic deformation to occur at the surface asperities of the substrate, at the boronizing temperature. The diffusion bonding of Ti6Al4V is generally performed at the pressures ranging from 1.3 MPa to 13.8 MPa (Donachie, 2000).

The SPB process is conducted in a vacuum furnace at a pressure of about 0.7 x 10^{-3} Pa. The temperature is raised and held up to 473 K for 10 minutes to remove the moisture before being raised to the final boronizing temperature. The heating process is conducted at a rate of 10°C / minute. The pressure inside the vacuum furnace is maintained throughout the whole heating cycle. After the process is completed, the specimen is cooled to a room temperature. Figure 3.9 shows the temperature and time profile of the boronizing process. The SPB process is carried out at three different temperatures of 1173 K, 1223 K, and 1273 K, and it is held for four different boronizing times of 1, 2, 3 and 6 hours. The times and temperatures used are listed in Table 3.2.

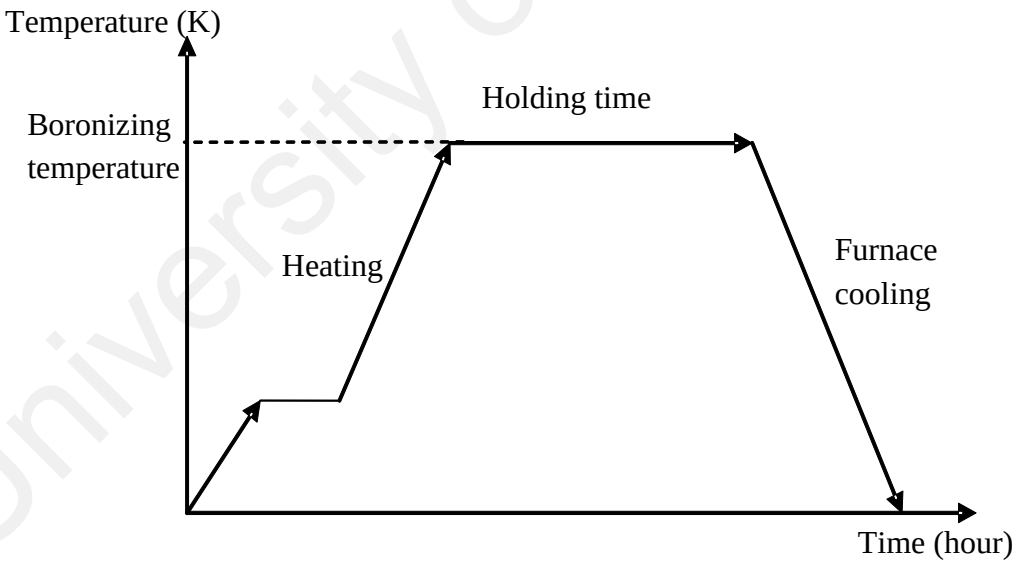

Figure 3.9 : Temperature and time profile of the boronizing process.

Table 3.2 : Temperature and time condition for SPB process.

No. of sample	Temperature (K)	Time (hour)
1	1173	1
2		2
3		3
4		6
5	1223	1
6		2
7		3
8		6
9	1273	1
10		2
11		3
12		6

3.5.1 Derivation of Load from Torque Unit to Stress

The initial pressure value is provided by tightening the clamp using a torque wrench. This section explains the derivation of load from a torque unit to a stress. Figure 3.10 shows a schematic diagram of the torque applied on the screws and Figure 3.11 shows a square-threaded power screw having a mean diameter *d*, a pitch *p*, and lead angle λ is loaded by an axial compressive force F.

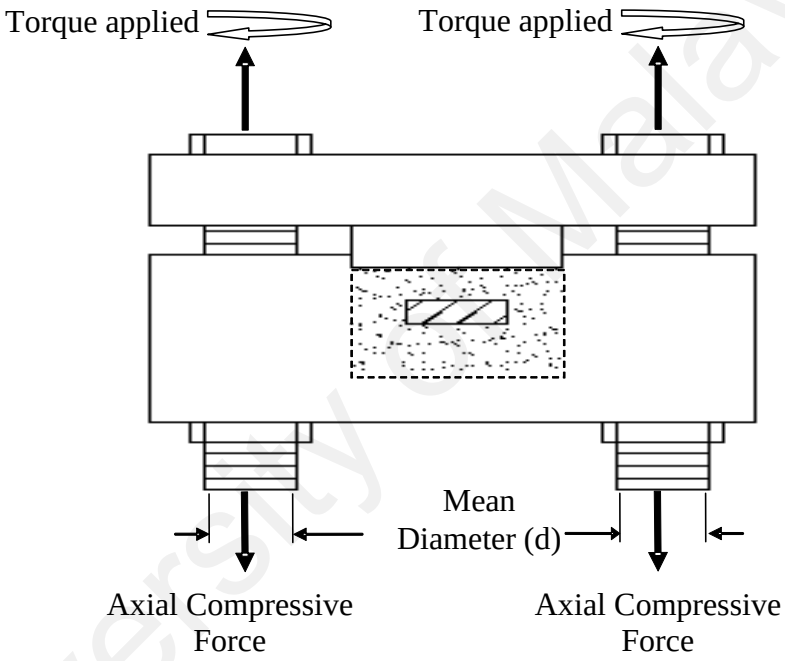

Figure 3.10 : The schematic diagram of the torque applied on the screws.

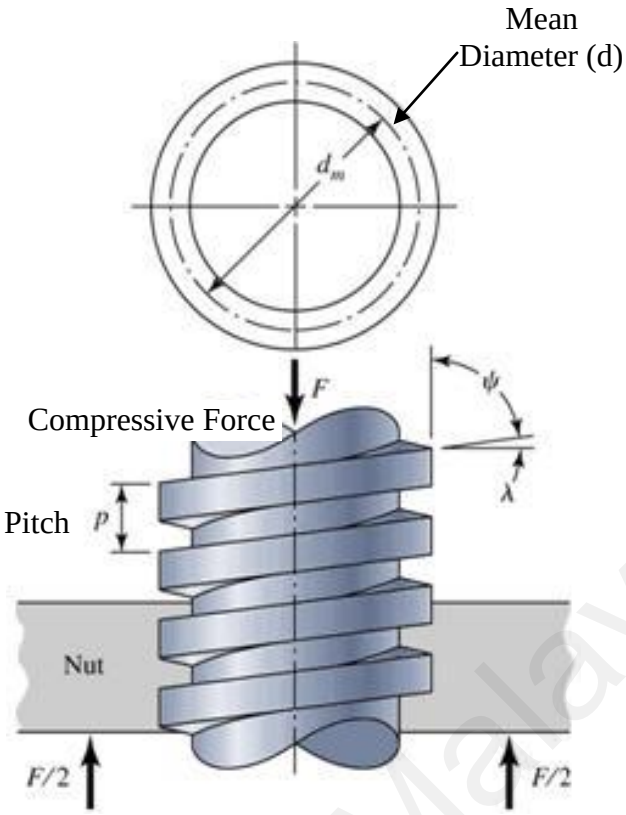

Figure 3.11 : Diagram of a square-threaded power screw with single thread (Nisbett & Budynas, 2014).

The relationship between torque (T) and compressive force (F) is (Nisbett & Budynas, 2014)

$$T = \frac{F\,d}{2}\left(\frac{\ell + \pi\,\mu\,d}{\pi d - \mu\ell}\right) \qquad \textbf{(3.1)}$$

where

T= Torque applied,

d = Mean diameter of the screw,

F = Compressive force,

ℓ = Thread length, and

μ = Coefficient of friction.

In this work, a type of screw M8 with black oxide coating is used. The screw has a mean diameter (d) of 8.8 mm and a coarse thread with the length (ℓ) of 1.25 mm (Oberg & Press, 2012). While the coefficient of friction of the screw is about 0.2 (Mortensen, 2013).

Therefore, from the Equation 3.1, the compressive force loaded on each screw is 54 kN. Figure 3.12 shows the free body diagram of the upper block of the clamp, subjected to the forces exerting on it.

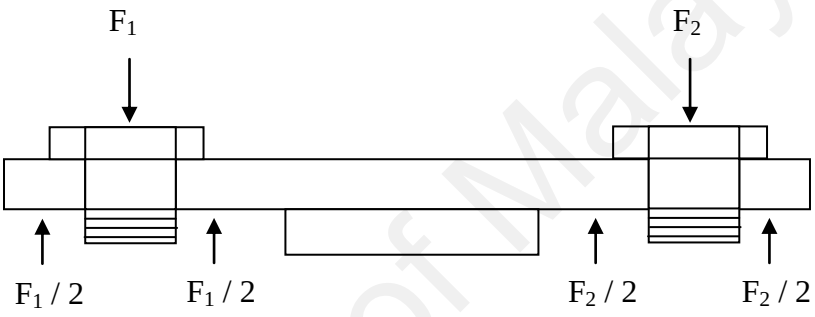

Figure 3.12 : Free body diagram of the upper block.

According to the Newton's third law, it is implied that all forces occur in pairs. If a body A exerts a force on a body B, than the body B exerts a force on the body A (Lambourne, 2000). Thus in this case, the forces that exerted to the puncher are F_1 / 2 and F_2 / 2 as illustrated in Figure 3.13.

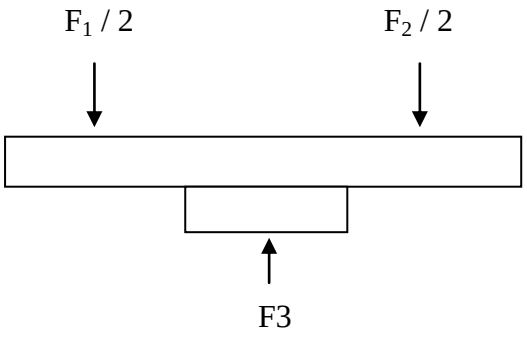

Figure 3.13 : Equilibrium force of the upper block.

Hence the total forces ($\frac{F1}{2}$) and ($\frac{F2}{2}$) is equal to F3.

$$\frac{F1}{2} + \frac{F2}{2} = F3 \qquad (3.2)$$

To obtain the initial pressure value, the initial load (F3) is divided by the area (A) of the puncher which contacts with the surface of the pack of powders as shown in Equation 3.3.

$$P = \frac{F3}{A} \qquad (3.3)$$

In this work, the surface area of the puncher is 165 mm^2 . Therefore from the Equation 3.3, the initial pressure value is 333 MPa. Table 3.3 shows the calculated value of initial load and pressure from the applied torque of 6 kgf.m.

Table 3.3 : Torque, initial load and pressure calculated values.

Torque (kgf.m)	Torque (N.m)	Load F_1 or F_2 (N)	Total F3 (N)	Initial pressure (MPa)
6	58.84	54043	54043	333

It is noted that the actual pressure value may be differ during the heating at a high temperature. Moreover, this is a theoretical value and been used to certify that the minimum pressure applied is sufficient for a deformation to occur at the surface asperities only. As mention earlier, the diffusion bonding of Ti6Al4V is generally performed at the pressures ranging from 1.3 MPa to 13.8 MPa (Donachie, 2000).

3.6 Characterization Methods

X-ray diffraction (XRD) analysis is performed on the specimens before and after the boronizing process to confirm the presence of boride phase. The microstructure and boronized layer thickness are analyzed using a scanning electron microscope (SEM). While the surface hardness is determined using a Vickers hardness tester.

3.6.1 X-ray Diffraction Analysis

X-ray Diffraction (XRD) is a one type of experimental tool to indentify the structure of crystalline solids. XRD is a versatile and non-destructive technique used for indentifying the crystalline phases present in solid materials and powders and for analyzing structural properties such as stress, grain size, phase composition, crystal orientation, and defect of the phases.

3.6.2 Scanning Electron Microscope (SEM)

Scanning Electron Microscope (SEM) is use to enlarge the image of the objects and allows a wealth of information to be obtained. It is used a focused beam of electrons instead of light to image the specimen and gain information as to its structure and composition.

The SEM has a large depth of field, which allows a large amount of the sample to be in focus at one time. It is also produces images of high resolution in which it can examines at a high magnification.

3.6.3 Microhardness Tester

The hardness test is available as a relatively simple alternatively to a tensile test. The resistance of a material to indentation is a qualitative indication of its strength. The term microhardness test usually refers to a static indentations made with a loads not

exceeding 10 N. In this work, the indenter used is the Vickers diamond pyramid at a load of HV 0.2 for 10 s. The procedure for testing is very similar to that of the standard Vickers hardness tester — the size of indentation is measured and converted to a hardness value, except that it is done on a microscopic scale with a higher precision instruments. Noted that, the hardness test is performed at five different points of surface for each specimen and the average hardness value is calculated.

CHAPTER 4 : RESULTS AND DISCUSSIONS

4.1 XRD Analysis and Surface Hardness

Figure 4.1 demonstrates the X-ray diffraction patterns of the Ti6Al4V surface before and after boronizing for 1 and 3 hours. From the relative peak intensity in the XRD pattern, only one type of borides, which is TiB_2, is identified after boronizing for 1 and 3 hours with the peak corresponding to the (100), (101) and (200) lattice planes respectively (Qin, Liu, Yang, & Tang, 2013; B. Sarma et al., 2012). TiB, which is also one of the commonly formed boride during the boronizing process, is not even identified here. The formation of TiB is skipped during this SPB process — as it will be discussed in the following section later.

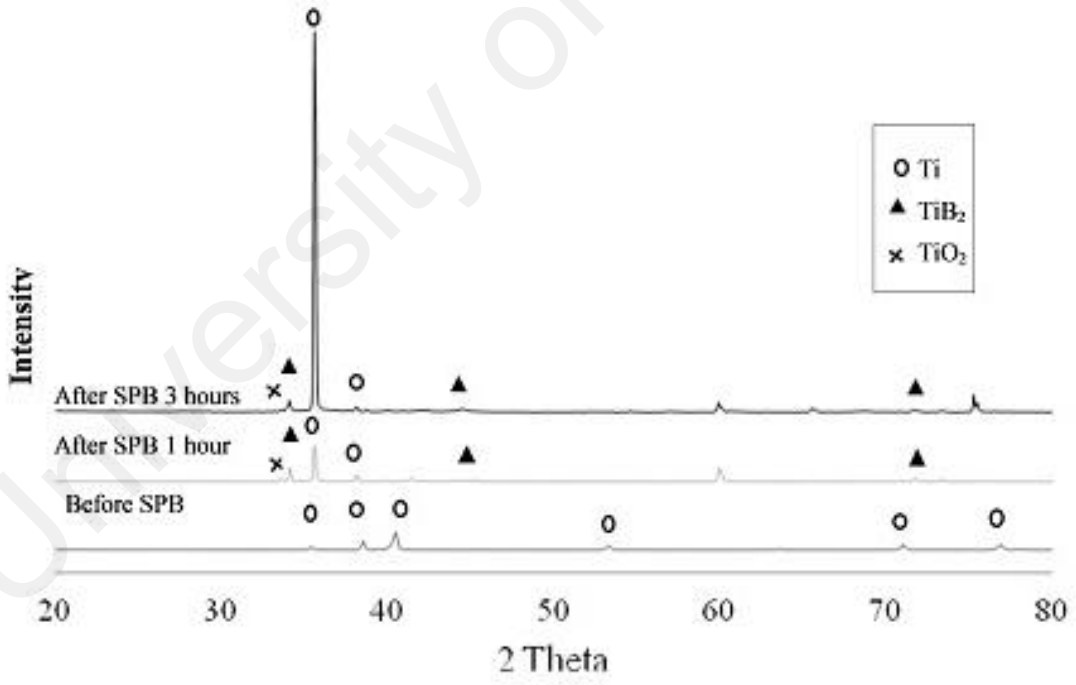

Figure 4.1 : X -ray diffraction patterns of Ti6Al4V before and after SPB for 1 hour to 3 hours at 1173 K.

From the figure, note also that — although the numbers of peaks are fewer than before the boronizing — Ti peaks are still being observed even after 3 hours of boronizing. This indicates that the surface is not yet completely covered with the TiB_2. The average particle size of 45 μm of boron powder is relatively huge compared to the average Ra of 0.01 μm. Therefore, at certain areas the substrate is not fully contacted with the boron powder.

Table 4.1 and Figure 4.2 show the surface hardness values of the specimens before and after boronizing. The surface hardness increase from 281 HV before boronizing to 1176, 1595, 1953 and 2047 HV after 1,2,3 and 6 hours of boronizing at 1173 K respectively. The increase in surface hardness with time suggests the formation's degree of the hard boride layer on the substrate surface.

Table 4.1 : Average hardness value (HV) of Ti6Al4V before and after SPB for 1 hour and 3 hours at 1173 K.

Boronizing time (hour)	(Before boronizing)	1	2	3	6
Average hardness (HV)	281	1176	1595	1953	2047

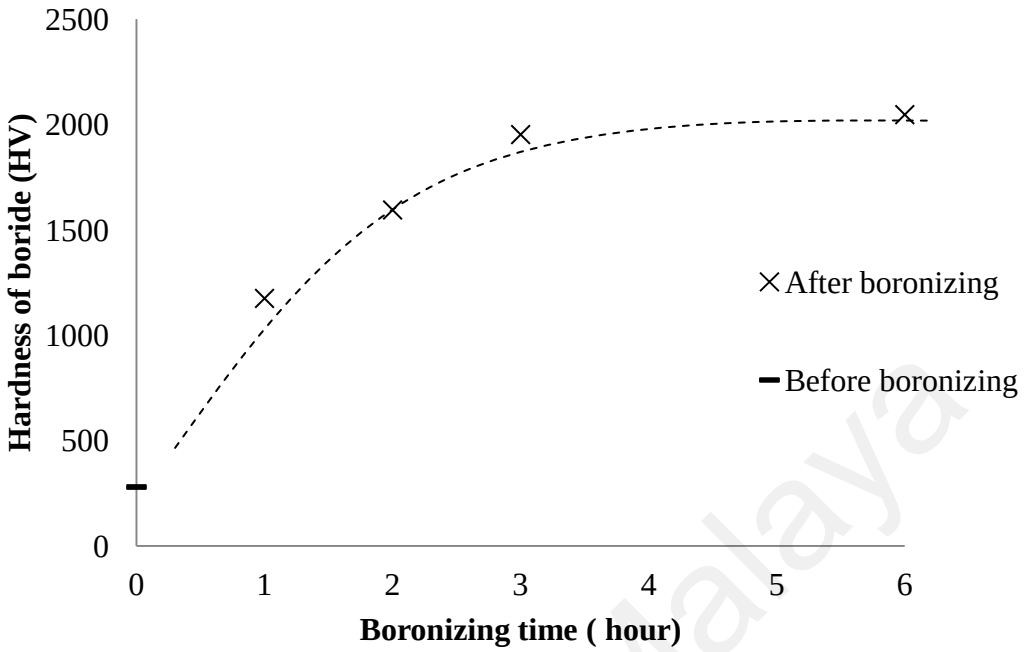

Figure 4.2 : Surface hardness (HV) of Ti6Al4V before and after boronizing at 1173 K.

4.2 Microstructure and Boronized Layer Thickness

Figure 4.3 shows the microstructure image of the substrate before the boronizing process. The average grain size of the substrate is measured as 9.6 μm. The micrograph showing a bi-modal microstructure consists of primary α surrounded by transformed β (Widmanstatten structure). Ti6Al4V is well known for its potential as the superplastic materials because the microstructure is composed by the two crystal structures of α and β structure.

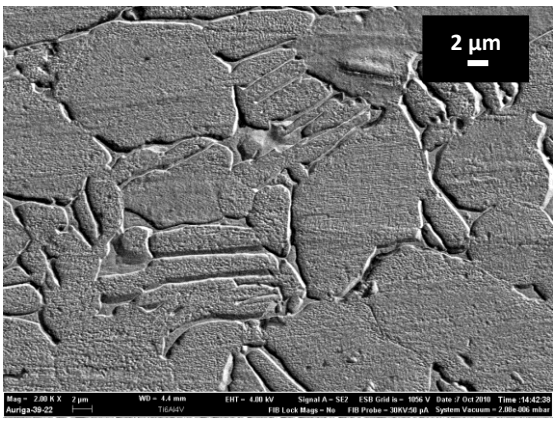

Figure 4.3 : Microstructure image of as-received Ti6Al4V.

Figure 4.4, 4.5 and 4.6 show the microscopy image of cross-section view of TiB_2 layer for SPB process at temperatures 1223 K, 1273 K and 1323 K for various times. As can be seen from the Figure 4.7, the plot of boronized layer thickness versus time, the boronized layer obviously increases with time, from 44.9 µm to 149.3 µm. The layer thickness obtained is tabulated in Table 4.2.

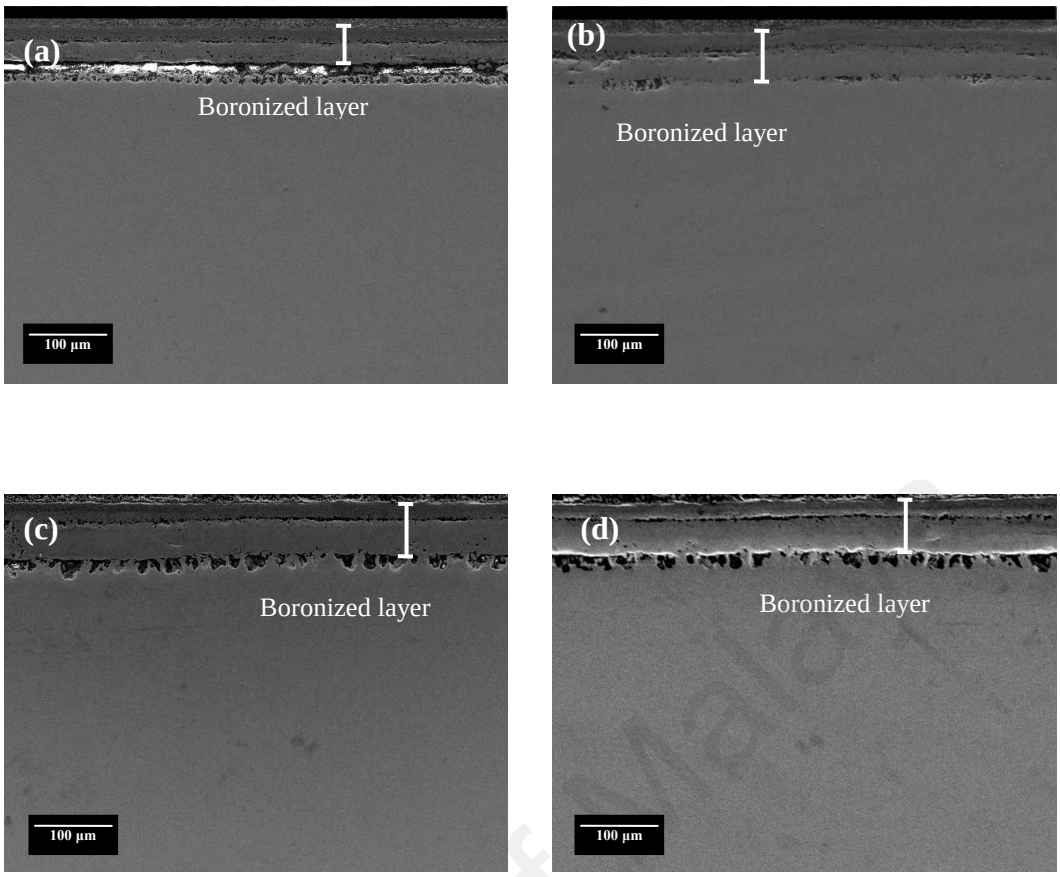

Figure 4.4 : SEM images of cross-sectional view of SPB Ti6Al4V at 1173 K for (a) 1 h (b) 2 h (c) 3 h and (d) 6 h.

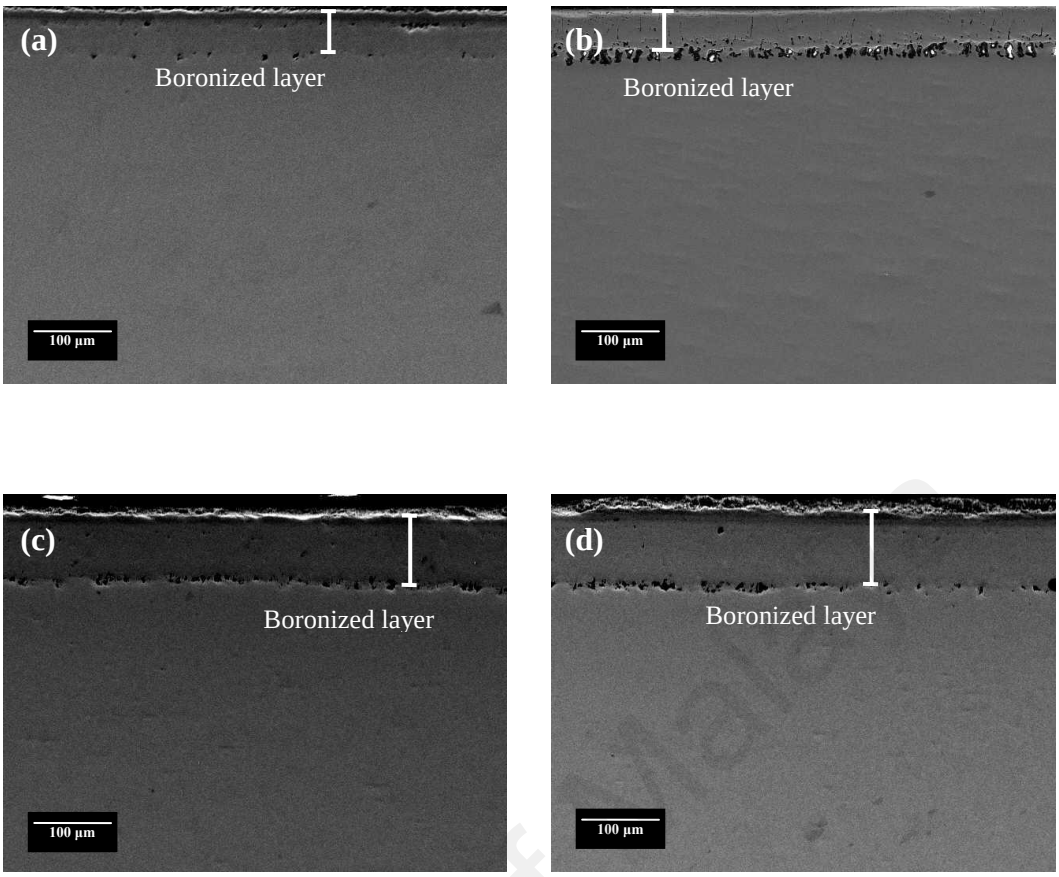

Figure 4.5 : SEM images of cross-sectional view of SPB Ti6Al4V at 1223 K for (a) 1 h (b) 2 h (c) 3 h and (d) 6 h.

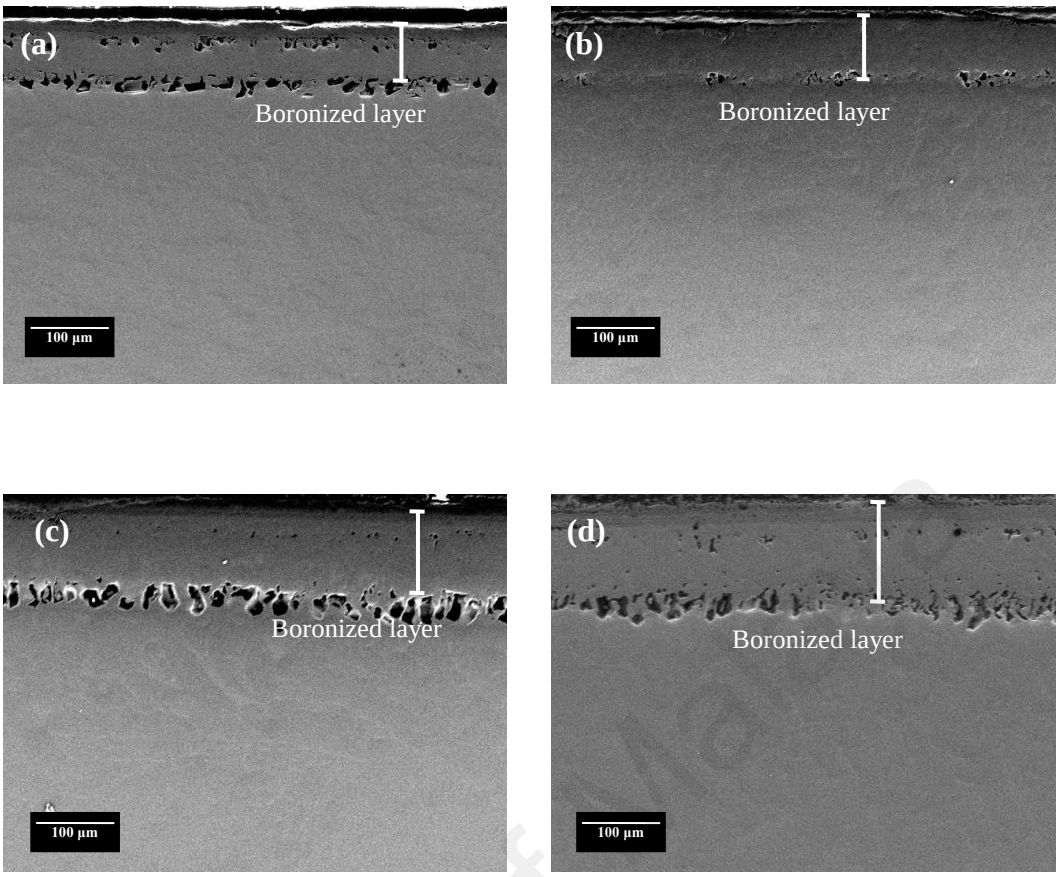

Figure 4.6 : SEM images of cross-sectional view of SPB Ti6Al4V at 1273 K for (a) 1 h (b) 2 h (c) 3 h and (d) 6 h.

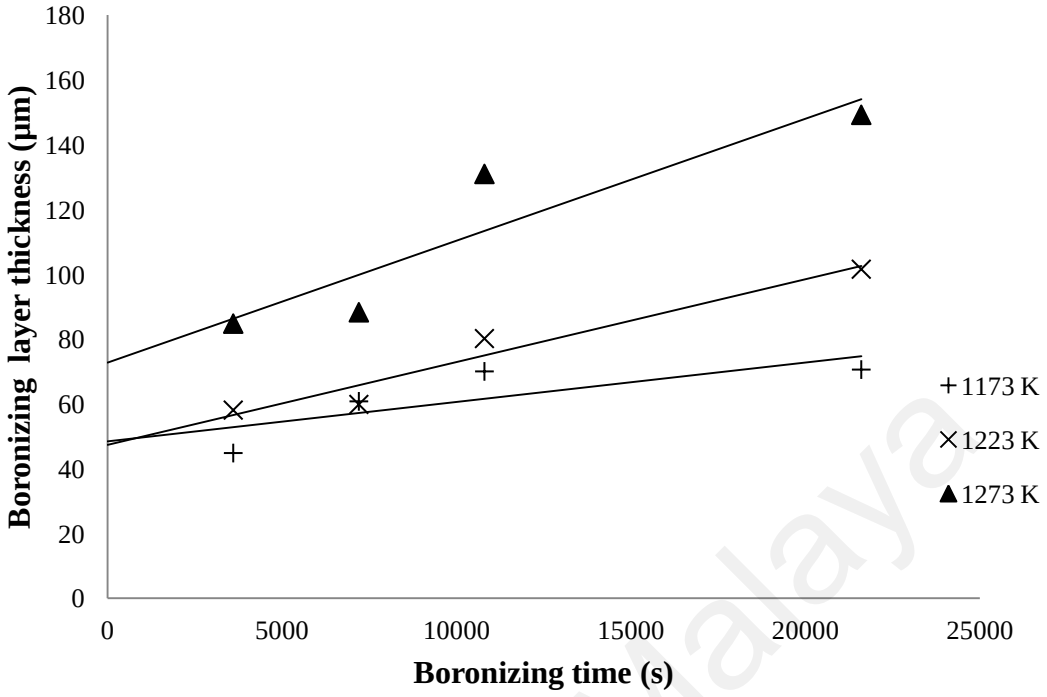

Figure 4.7 : TiB_2 layer thickness (µm) vs boronizing time (s).

Table 4.2 : Average boronized layer thickness (µm) at various treatment temperatures.

Temperature (K)	Time (hour)	Average boronized layer thickness (µm)
1173	1	44.9
	2	60.8
	3	70.1
	6	70.7
1223	1	58.1
	2	59.9
	3	80.2
	6	101.6
1273	1	84.8
	2	88.3
	3	131
	6	149.3

4.3 Characteristic of Boronized Layer

Figure 4.8 shows the cross sectional view of the specimen boronized at 1273 K for 1 to 6 hours. From the figure, note that a set of layers is formed on the substrate's surface area. The layers can be differentiated as (I) boronized layer, (II) discontinuous pore layer and (III) the substrate.

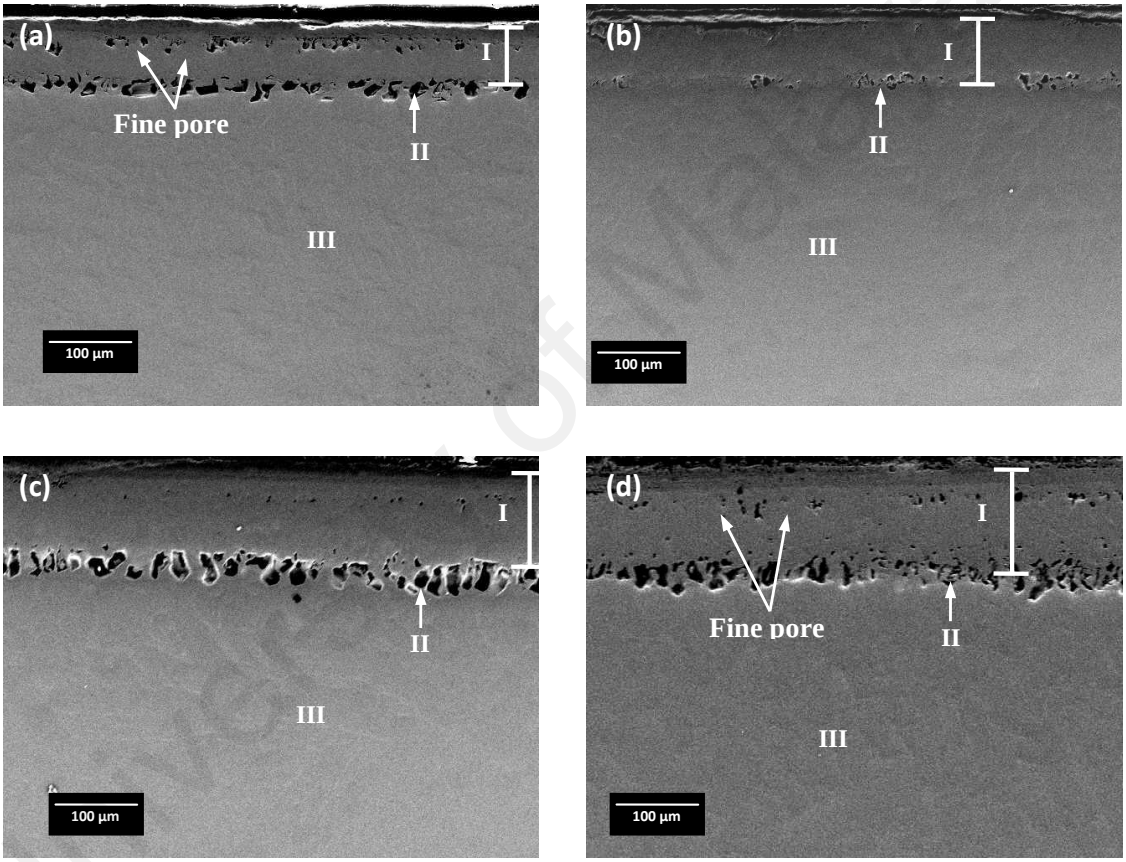

Figure 4.8 : SEM images of cross-sectional view of SPB Ti6Al4V at 1273 K for (a) 1 h (b) 2 h (c) 3 h and (d) 6 h.

The existence of fine pores is also noticeable in some areas of the boronized layer (Figure 4.8 (a) and (d)), however, in some other areas the fine pores are almost un-noticeable (Figure 4.8 (b) and (c)).

Below the boronized layer, a layer of discontinuous with bigger pores is seen. The discontinuous pores layer is formed as a result of the movement of atoms, especially aluminium (Al) from the area close to the boronized layer to the core of the substrate. With the introduction of boron into the substrate, TiB_2 will obviously be formed. Al with relatively smaller in size as compared to titanium (Ti) and vanadium (V), cannot dissolve in TiB_2 component thus tend to move away (Li et al., 2010). This can be confirmed from the EDS line scanning profile of Al in Figure 4.9, where the intensity of Al in the boronized layer is obviously low at a depth of 0 to about 30 μm, however it is increased at about 30 to 60 μm depth before stabilizes at 70 μm depth. As suggested, this profile shows that Al atoms tend to move to the core of the substrate as well as boronized layer forms. However in its path, the Al atoms get accumulated - as indicated by the increase in Al intensity - as it couldn't move further. The existence of the aforementioned fine pores in the boronized layer also might be attributed to this phenomenon, but in a much lesser degree and uniformity. The phenomenon is a kind of Kirkendall effect that occurs as a consequence of the difference in a diffusion rate in the alloy (Bhadeshia, 2013). In certain areas, although the fine pores in the boronized layer region and the discontinuous pores layer are relatively not so clear (as in Figure 4.8 (b)), the three main layers are still distinguishable. The formation of pores is also seen elsewhere (Tsipas et al., 2010). Although it is beyond the scope of this study, these pores can be eliminated through a high temperature annealing after the boronizing process.

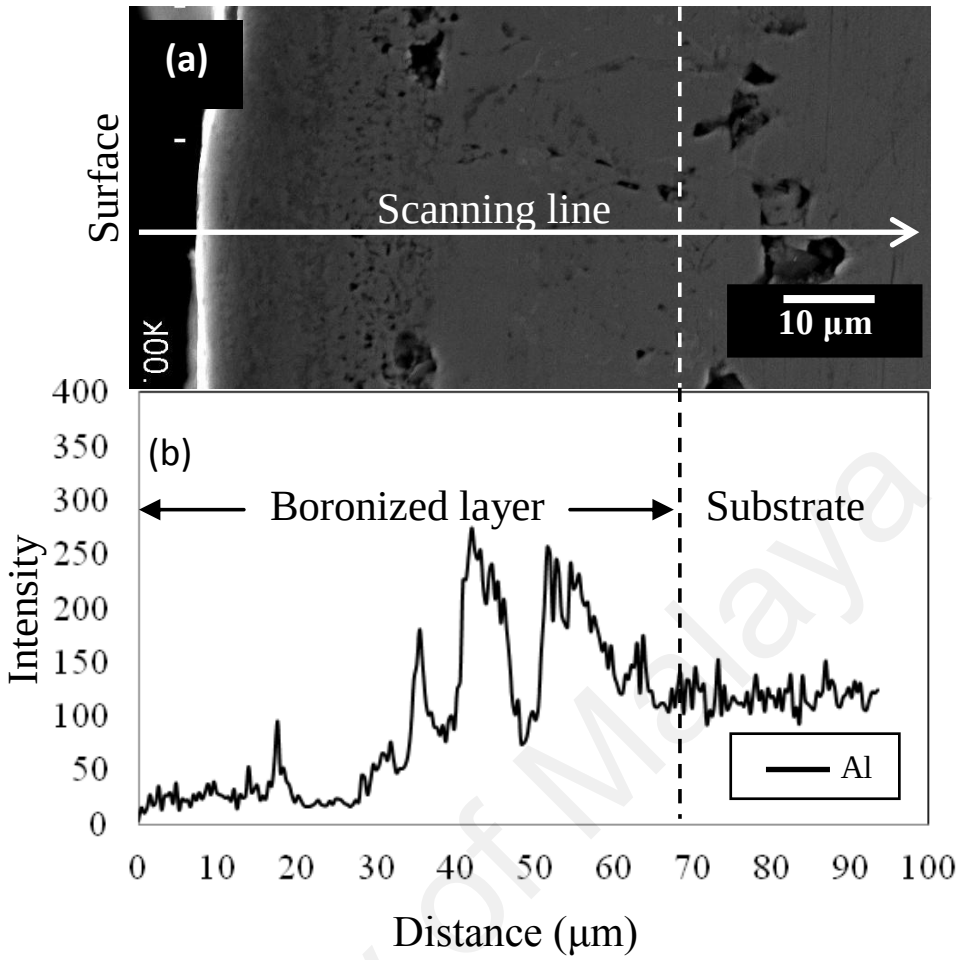

Figure 4.9 : (a) SEM image of cross-sectional view and (b) EDS line scanning profile of Al for boronized Ti6Al4V at 1173 K (900 ^{0}C) for 6 hours.

The boronized layer thickness and surface hardness of the substrate increase with the boronizing time and temperature. As more boron atoms diffuse into the substrate, the boronized layer thickness increase respectively and the surface hardness is also expected to increase. Table 4.3 shows the diffusion coefficient values at each temperature. The diffusion coefficient values of all temperatures can be determined by the slope of the straight line from the plot of square of boronized layer thickness versus time as shown in the Figure 4.10. The diffusion coefficient values obtained are 1.44 x 10^{-13}, 4.1 x 10^{-13} and 8.86 x 10^{-13} m^2s^{-1} respectively. This is higher as compared with the other works (Li et al., 2010; Tikekar et al., 2007) shown in Table 4.4. The

higher diffusion coefficient values achieved suggests that the role of SPB crucially played in the process. Through the superplastic deformation of the surface asperities and diffusion of atoms into the fine grains, the diffusion of boron atoms into the substrate is accelerated. It is also interesting to note that the diffusion coefficient values obtained are at the lower temperature range than in the works reported.

Table 4.3 : The diffusion coefficient values obtained for various treatment temperatures.

Temperature (K)	Time (hour)	Diffusion coefficient (m^2/s)
1173	1	1.44×10^{-13}
	2	
	3	
	6	
1223	1	4.10×10^{-13}
	2	
	3	
	6	
1273	1	8.86×10^{-13}
	2	
	3	
	6	

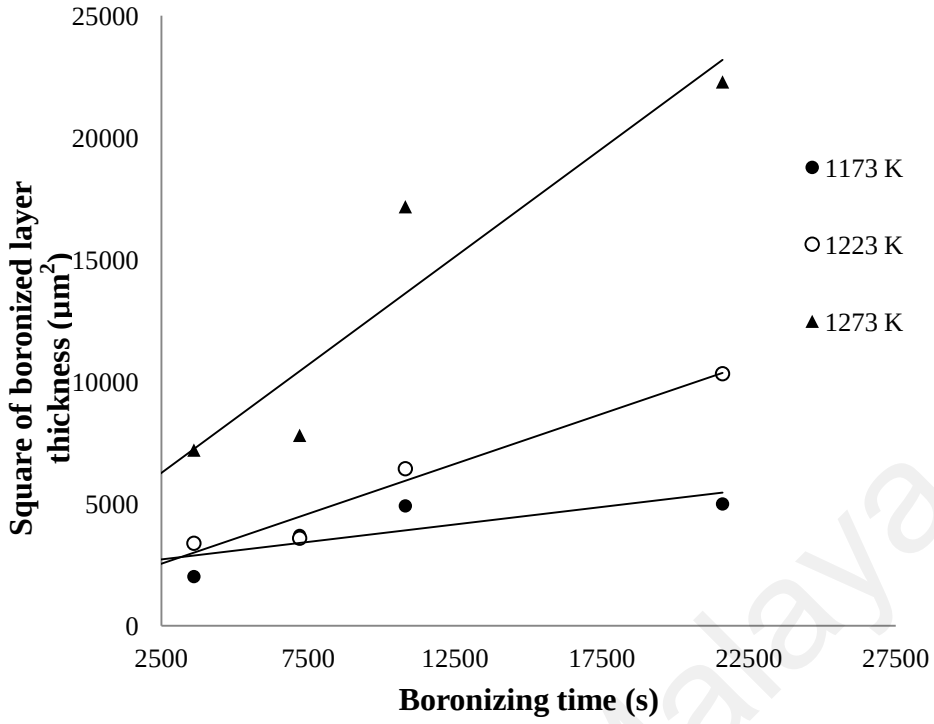

Figure 4.10 : Square of TiB_2 layer thickness (μm^2) vs boronizing time (s).

Table 4.4 : The diffusion coefficient values of boron into Ti/Ti alloy in some references.

Boronizing technique	Base material	Process condition		Diffusion coefficient (m^2/s)	Reference
		Temperature (K)	Time (hr)		
Pack boriding	Ti	1173 - 1323	3-24	*(2.2 - 2.86) x 10^{-14}	(Tikekar et al., 2007)
Pack boriding	Ti6Al4V	1273-1373	5-20	(1.95 - 3.06) x 10^{-15}	(Li et al., 2010)

***The diffusion coefficient value is calculated from the reported result.**

As mentioned earlier, a high diffusion rate process of boron atoms into Ti is required for boride to achieve its saturated composition of TiB_2. In this work, since only TiB_2 is detected, it suggests that the SPB has able to skip the TiB formation thus creating a more desirable process.

4.4 Activation energy determination

The thickness of the boronized layer varies with time and follows the parabolic law as below:

$$d^2 = Kt \qquad (4.1)$$

Where d is the boronized layer thickness (m), t is the boronizing time (s) and K is the boride growth rate constant or diffusion coefficient of boron into the matrix. Figure 4.10 indicates that the square of boronized layer thickness changes linearly with time.

Therefore, the relationship between the diffusion coefficients, K (m^2s^{-1}), activation energy, Q (J Mol^{-1}) and boronizing temperature, T (K) can be expressed by the Arrhenius equation as follows:

$$K = K_o\, e^{-(Q/RT)} \qquad (4.2)$$

where K_o is the pre-exponential constant and R is the gas constant (8.314 $Jmol^{-1}K^{-1}$). Taking the natural logarithm of Equation 4.2, Equation 4.3 can be derived as follows:

$$\ln K = \ln K_o + (-QR^{-1})(T^{-1}) \qquad (4.3)$$

As shown in Figure 4.11, the plot of the natural logarithm of the boride growth rate (ln K) versus the reciprocal of the boronizing temperature (T^{-1}) for the SPB is linear. Thus, the slope of the straight line will determine the activation energy (Q) of the boronizing process. From Figure 4.11, the activation energy for the SPB is determined as 226.17 $kJmol^{-1}$. The activation energy value obtained in this study, declares the activity of the boron and titanium at the given temperatures range. The value is higher as compared to the previous work (Li et al., 2010), but since the temperature range is different, a direct comparison is difficult to make.

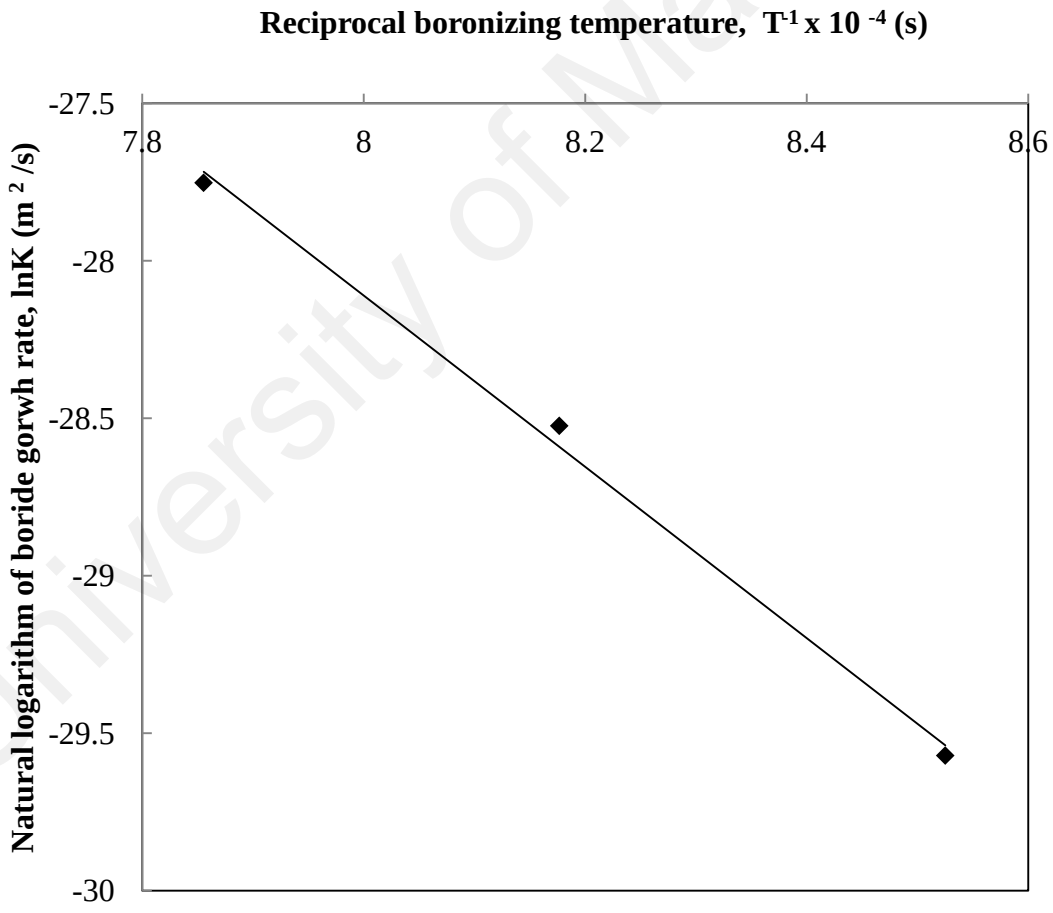

Figure 4.11 : Natural logarithm of boride growth rate ln K vs. reciprocal boronizing temperature (T^{-1}).

From the results of this study, it shows that the SPB can be implemented in the boronizing of titanium. Through the SPB, much higher boronized layer thickness value (up to 149 μm) can be obtained. The SPB helps to make the boronizing process more efficient with faster process rate. With such positive prospects, further studies are required in the future to evaluate specifically the properties of the boronized layer (especially wear property) for the actual industrial applications.

CHAPTER 5 : CONCLUSIONS AND RECOMMENDATIONS

5.1 Conclusions

The superplastic boronizing of Ti6Al4V has been conducted in this work and the following conclusions are obtained:

1. Boride phase identified as TiB_2 is detected without any sign of TiB.

2. Three layers of boronized layer, discontinuous pores layer and substrate layer are formed after the boronizing process.

3. Boronized thickness layer in the range of 44.9 to 149.3 μm is formed on the surface of Ti6Al4V after SPB.

4. Kirkendall like phenomenon creates a discontinuous pore layer as a result of the movement of Al atoms from the boride region.

5. Diffusion coefficient values obtained are 1.44×10^{-13}, 4.1×10^{-13} and 8.86×10^{-13} m^2s^{-1} respectively which is higher as compared with the other works reported.

6. Activation energy for the SPB process is 226.17 $kJmol^{-1}$.

5.2 Recommendations

Some considerations and developments can be suggested for further investigation in the mechanical properties and improvement of the boronized layer as follows:

1) Mechanical testing such as wear and scratch test should be studied to determine the adhesion strength between the boronized layer and the substrate.

2) Further treatment such as annealing process has to be conducted in order to minimize and eliminate the formation of many voids that was discussed in the previous section hence increase the mechanical properties of the boronized layer.

3) The critical issue for this study is the formation of the voids at the interface area between the boronized layer and the substrate. Therefore, it is crucial to measure the cross sectional hardness of the boronized layer from the surface down to the substrate. It is recommended to conduct the nanoindentation testing by indenting to a depths at the nanometer-micron scales. The test will provide the surface mechanical characterization data and should be useful for further investigation.

4) Another interesting area to study is the application of the produced material and its potential usage in the industry

REFERENCES

Ahamad, N., & Jauhari, I. (2012). Carburizing of Duplex Stainless Steel (DSS) Under Compression Superplastic Deformation. *Metallurgical and Materials Transactions A, 43*(13), 5115-5121. doi: 10.1007/s11661-012-1357-4

Atar, E., Kayali, E. S., & Cimenoglu, H. (2008). Characteristics and wear performance of borided Ti6Al4V alloy. *Surface and Coatings Technology, 202*(19), 4583-4590. doi: http://dx.doi.org/10.1016/j.surfcoat.2008.03.011

Azis, S. A. A., Jauhari, I., Masdek, N. R. N., Ahamad, N. W., & Ogiyama, H. (2010). Surface Roughness and Initial Pressure Effect on Superplastically Carburized Duplex Stainless Steel. *Defect and Diffusion Forum, 297-301*, 227-232.

Bhadeshia, H. K. D. H. (2013). Kiekendall Effect. www.msm.cam.ac.uk/phase- tr ans/ki r kendal l .html

Bhaumik, S. K., Divakar, C., Singh, A. K., & Upadhyaya, G. S. (2000). Synthesis and sintering of TiB2 and TiB2–TiC composite under high pressure. *Materials Science and Engineering: A, 279*(1–2), 275-281. doi: http://dx.doi.org/10.1016/S0921-5093(99)00217-8

Bloor, D., Brook, R. J., Flemings, M. C., & Mahajan, S. (1994). The encylopeia of advance materials. *Elsevier Science Ltd., 4*, 2712-2722.

Chakrabarty, J. (2010). *Applied Plasticity, Second Edition*: Springer US.

Chandra, N. (2002). Constitutive behavior of superplastic materials. *International journal of non-linear mechanics, 37*(3), 461-484.

Chaturvedi, M. C. (2011). *Welding and Joining of Aerospace Materials*: Elsevier Science.

Conway, B. E. (2006). *Modern Aspects of Electrochemistry, Number 38: No. 38*: Springer London, Limited.

Donachie, M. J. (2000). *Titanium: A Technical Guide, 2nd Edition*: ASM International.

Driver, P. G. F. T. J. H. (1981). Surface treatment of steels: Borudif, a new boriding process. *Thin Solid Films, 78*(1), 67-76.

El Mel, A.-A., Nakamura, R., & Bittencourt, C. (2015). The Kirkendall effect and nanoscience: hollow nanospheres and nanotubes. *Beilstein Journal of Nanotechnology, 6*, 1348-1361. doi: 10.3762/bjnano.6.139

Friedman, P. A., & Luckey, S. G. (2004). On the Expanded Usage of Superplastic Forming of Aluminium Sheet for Automotive Applications. *Materials Science Forum, 447-448*, 199-204.

Genel, K., Ozbek, I., & Bindal, C. (2003). Kinetics of boriding of AISI W1 steel. *Materials Science and Engineering: A, 347*(1), 311-314. doi: 10.1016/S0921-5093(02)00607-X

Gifkins, R. C. (1976). Grain-boundary sliding and its accommodation during creep and superplasticity. *Metallurgical Transactions A, 7*(8), 1225-1232. doi: 10.1007/BF02656607

Giuliano, G. (2011). *Superplastic Forming of Advanced Metallic Materials: Methods and Applications*: Elsevier Science.

Han, W., Zhang, K., Wang, G., & Zhang, X. (2005). Superplastic Forming and Diffusion Bonding for Sandwich Structure of Ti-6Al-4V Alloy. *材料科学技术学报 (英文版, 21*(1).

Hanliang Zhu, B. Z., Zhiqiang Li and Kouichi Maruyama. (2005). Superplasticity and Superplastic Diffusion Bonding of a Fine-Grained TiAl Alloy. *Materials Transactions, 46*(10), 2150-2155.

Hasan, R. (2006). *Development of superplastic boronizing using duplex stainless steel.* (Master Dissertation), University of Malaya.

Hasan, R., Jauhari, I., Ogiyama, H., & Ramdan, R. D. (2006). Effects of Superplasticity in Boronizing of Duplex Stainless Steel. *Key Engineering Materials, 326-328*, 1233-1236.

Hertzberg, R. W. (1996). *Deformation and fracture mechanics of engineering materials*: J. Wiley & Sons.

Jain, V., & Sundararajan, G. (2002). Influence of the pack thickness of the boronizing mixture on the boriding of steel. *Surface and Coatings Technology, 149*(1), 21-26. doi: 10.1016/S0257-8972(01)01385-8

Jauhari, I., Ogiyama, H., & Tsukuda, H. (2003). Solid State Diffusion Bonding of Superplastic Duplex Stainless Steel with Carbon Steel. *Journal of the Society of*

Materials Science, Japan, 52(6Appendix), 154-159. doi: 10.2472/jsms.52.6Appendix_154

Jauhari, I., Yusof, H. A. M., & Saidan, R. (2011). Superplastic boronizing of duplex stainless steel under dual compression method. *Materials Science and Engineering: A, 528*(28), 8106-8110. doi: http://dx.doi.org/10.1016/j.msea.2011.07.054

Kum, D. W., Oyama, T., Sherby, O. D., Ruano, O. A., & Wadsworth, J. (Eds.). (1984). *1984*: Metal Park.

Lambourne, R. (2000). *Predicting Motion*: Taylor & Francis.

Langdon, T. G. (1970). Grain boundary sliding as a deformation mechanism during creep. *Philosophical Magazine, 22*(178), 689-700.

Li, F., Yi, X., Zhang, J., Fan, Z., Gong, D., & Xi, Z. (2010). Growth kinetics of titanium boride layers on the surface of Ti6Al4V. *Acta Metallurgica Sinica (English Letter), 23*(4), 293-300.

Lutfullin, R. Y., Imayev, R.M., Kaibyshev, O.A., Hismatullin, F.N. and Imayev, V.M. (1995). Superplasticity and solid state bonding of the TiAl intermetallic compound with micro- and submicrocrystalline structure. *Scripta Metallurgica et Materialia, 33*(9), 1445-1449.

Lütjering, G. (1998). Influence of processing on microstructure and mechanical properties of (α+ β) titanium alloys. *Materials Science and Engineering: A, 243*(1), 32-45.

Matsushita, M. (2011). Boronization and Carburization of Superplastic Stainless Steel and Titanium-Based Alloys. *Materials, 4*(7), 1309.

Mortensen, J. (2013). Friction Analysis of Bolts (pp. 33). Aalborg Universitet Esbjerg: Arvid Nilsson, Kolding.

Mukherjee, A. K. (1971). The rate controlling mechanism in superplasticity. *Materials Science and Engineering, 8*(2), 83-89.

Munro, R. G. (2000). Material properties of titanium diboride. *Journal of Research of the National Institute of Standards and Technology, 105*(5), 709-720.

Murray, J. L., Liao, P. K., & Spear, K. E. (1986). The B−Ti (Boron-Titanium) system. *Bulletin of Alloy Phase Diagrams, 7*(6), 550-555.

Murthy, T. S. R. C., Sonber, J. K., Subramanian, C., Hubli, R. C., Krishnamurthy, N., & Suri, A. K. (2013). Densification and oxidation behavior of a novel TiB2–MoSi2–CrB2 composite. *International Journal of Refractory Metals and Hard Materials, 36*(0), 243-253. doi: http://dx.doi.org/10.1016/j.ijrmhm.2012.09.006

Natali, A. N. (2003). *Dental Biomechanics*: CRC Press.

Nisbett, K., & Budynas, R. (2014). *Shigley's Mechanical Engineering Design*: McGraw-Hill Education.

Oberg, E., & Press, I. (2012). *Section 05. Tooling and Toolmaking – Machinery's Handbook 29*: Industrial Press.

Polmear, I. (1981). *Light Alloys*. London: Edward Arnold Publishers Ltd.

Qin, L., Liu, C., Yang, K., & Tang, B. (2013). Characteristics and wear performance of borided Ti6Al4V alloy prepared by double glow plasma surface alloying. *Surface and Coatings Technology, 225*(0), 92-96. doi: http://dx.doi.org/10.1016/j.surfcoat.2013.02.053

Rosen, A., Arieli, A., & Mukherjee, A. K. (1980). A model for the rate-controlling mechanism in superplasticity. *Material Science and Engineering, 45* (1), 61-70.

Russell, A., & Lee, K. L. (2005). *Structure-Property Relations in Nonferrous Metals*: Wiley.

Sarma, B. (2011). Accelerated kinetics and mechanism of growth of boride layers on titanium under isothermal and cyclic diffusion.

Sarma, B., Tikekar, N. M., & Ravi Chandran, K. S. (2012). Kinetics of growth of superhard boride layers during solid state diffusion of boron into titanium. *Ceramics International, 38*(8), 6795-6805. doi: http://dx.doi.org/10.1016/j.ceramint.2012.05.077

Shangguan, D. (2005). *Lead-free Solder Interconnect Reliability*: ASM International.

Tikekar, N. M., Ravi Chandran, K. S., & Sanders, A. (2007). Nature of growth of dual titanium boride layers with nanostructured titanium boride whiskers on the surface of titanium. *Scripta Materialia, 57*(3), 273-276. doi: http://dx.doi.org/10.1016/j.scriptamat.2007.03.050

Totten, G. E., Funatani, K., & Xie, L. (2004). *Handbook of Metallurgical Process Design*: CRC Press.

Tsipas, S. A., Vázquez-Alcázar, M. R., Navas, E. M. R., & Gordo, E. (2010). Boride coatings obtained by pack cementation deposited on powder metallurgy and wrought Ti and Ti–6Al–4V. *Surface and Coatings Technology, 205*(7), 2340-2347. doi: http://dx.doi.org/10.1016/j.surfcoat.2010.09.026

Tsuzuku, T., Takahashi, A., & Sakamoto, A. (Eds.). (1991). *Application of superplastic forming for aerospace components*.

Vanderhasten, M., Rabet, L., & Verlinden, B. (2005). AME High temperature deformation of Ti6Al4V at low strain rate (Vol. 11, pp. 195-200): Association of Metallurgical Engineers of Serbia.

Wang, Z. R., & Zhang, K. F. (1988). *Superplasticity and Superplastic Forming*. Paper presented at the Development of superplastic forming technology in China.

Xing, H., Wang, C., Zhang, K., & Wang, Z. (2004). Recent development in the mechanics of superplasticity and its applications. *Journal of Materials Processing Technology, 151*(1), 196-202.

Xu, C. H., Xi, J. K., & Gao, W. (1996). Isothermal superplastic boronizing of high carbon and low alloy steels. *Scripta Materialia, 34*(3), 455-461. doi: http://dx.doi.org/10.1016/S0956-716X(95)00541-3

Xu, C. H., Xi, J. K., & Gao, W. (1997). Improving the mechanical properties of boronized layers by superplastic boronizing. *Journal of Materials Processing Tech., 65*(1-3), 94-98. doi: 10.1016/0924-0136(95)02247-3

Xun, Y. W., & Tan, M. J. (2000). Applications of superplastic forming and diffusion bonding to hollow engine blades. *Journal of Materials Processing Technology, 99*(1), 80-85. doi: 10.1016/S0924-0136(99)00377-5

Yapar, U., Basman, G., Arisoy, C.F., Yesilcubuk, S.A., Sesen, M.K. (2004). Influence of boronizing on mechanical properties of EN-C35E steel. *Key Engineering Materials, 264-268(pt.1)*, 629-632.

Yusof, H. A. M. (2010). *Superplastic boronizing of duplex stainless steel through dual compression method.* (Master), University of Malaya, University of Malaya.

Yusof, H. A. M. (2010). *Surface properties and kinetics of boronized DSS.* (Master Dissertation), University of Malaya.

Yusof, H. A. M., Jauhari, I., Rozali, S., & Hiroyuki, O. (2007). Effect Of Powder Particle Sizes On The Development Of Ultra Hard Surface Through Superplastic

Boronizing Of Duplex Stainless Steel. *Key Engineering Materials*, *345-346*, 601-604.

Zelin, M. G., & Mukherjee, A. K. (1996). Geometrical aspects of superplastic flow. *Materials Science and Engineering: A*, *208*(2), 210-225. doi: http://dx.doi.org/10.1016/0921-5093(95)10080-6

Zhao, G., Huang, C., Liu, H., Zou, B., Zhu, H., & Wang, J. (2014). Microstructure and mechanical properties of TiB2–SiC ceramic composites by Reactive Hot Pressing. *International Journal of Refractory Metals and Hard Materials*, *42*(0), 36-41. doi: http://dx.doi.org/10.1016/j.ijrmhm.2013.10.007

Internet References

URL: 1) http://www.azom.com/details.asp?ArticleID=915)

URL: 2) http://www.efunda.com/process/heat_treat/hardening/diffusion.cfm

LIST OF PUBLICATION AND CONFERENCE

JOURNAL

Nor Taibah Taazim , Iswadi Jauhari, Yukio Miyashita, Mohd Faizul Mohd Sabri (2016). Development and kinetics of TiB_2 layers on the surface of titanium alloy by superplastic boronizing. *Metallurgical and Materials Transactions A.* 1-6. doi: 10.1007/s11661-016-3359-0 (**Q1**)

CONFERENCE

Nor Taibah Taazim, Iswadi Jauhari (2012). Superplastic deformation effects on carburized Ti6Al4V. The 3rd Asian Symposium on Material & Processing (ASMP 2012). 30-31 August 2012. Chennai, India.